

Wright State University

CORE Scholar

---

[Browse all Theses and Dissertations](#)

[Theses and Dissertations](#)

---

2016

## Design and Application of Facile Routes to N-Heterocycle Functionalized Poly(arylene ether)s

Abraham K. Kemboi  
*Wright State University*

Follow this and additional works at: [https://corescholar.libraries.wright.edu/etd\\_all](https://corescholar.libraries.wright.edu/etd_all)

 Part of the [Chemistry Commons](#)

---

### Repository Citation

Kemboi, Abraham K., "Design and Application of Facile Routes to N-Heterocycle Functionalized Poly(arylene ether)s" (2016). *Browse all Theses and Dissertations*. 2042.  
[https://corescholar.libraries.wright.edu/etd\\_all/2042](https://corescholar.libraries.wright.edu/etd_all/2042)

This Thesis is brought to you for free and open access by the Theses and Dissertations at CORE Scholar. It has been accepted for inclusion in Browse all Theses and Dissertations by an authorized administrator of CORE Scholar. For more information, please contact [library-corescholar@wright.edu](mailto:library-corescholar@wright.edu).

**DESIGN AND APPLICATION OF FACILE ROUTES TO N-HETEROCYCLE  
FUNCTIONALIZED POLY(ARYLENE ETHER)S**

A thesis submitted in partial fulfillment  
of the requirements for the degree of  
Master of Science

By:

ABRAHAM K. KEMBOI

BEDs, Moi University, 2008

2015

Wright State University

WRIGHT STATE UNIVERSITY  
GRADUATE SCHOOL

July 30, 2015

I HEREBY RECOMMEND THAT THE THESIS PREPARED UNDER MY SUPERVISION BY Abraham K. Kemboi ENTITLED Design and Application of Facile Routes to N-Heterocycle Functionalized Poly(arylene ether)s BE ACCEPTED IN PARTIAL FULFILLMENT OF THE REQUIREMENTS FOR THE DEGREE OF Master of Science.

---

Eric Fossum, Ph.D.

Thesis Advisor

---

David Grossie, Ph.D.

Chair, Department of Chemistry

Committee on

Final Examination

---

Eric Fossum, Ph.D.

---

Daniel M. Ketcha, Ph.D.

---

William A. Feld, Ph.D.

---

Robert E. W. Fyffe, Ph.D.

Vice President for Research and

Dean of the Graduate School

## ABSTRACT

Abraham Kemboi M.S., Department of Chemistry, Wright State University, 2015. Design and Application of Facile Routes to *N*-Heterocycle Functionalized Poly(arylene ether)s

A series of 3,5-difluorinated systems, which are activated towards nucleophilic aromatic substitution (NAS) by the strongly electron withdrawing benzoxazole or benzothiazole groups, located *meta* to the fluorines were prepared and fully characterized. The monomers also carry various *N*-heterocyclic species on the non-fluorinated ring. The corresponding poly(arylene ether)s, some of which were copolymers with triphenylphosphine oxide-based monomers, were prepared via standard NAS polycondensation reactions. Incorporation of the monomers containing *N*-heterocycle units was determined by NMR spectroscopy. Characterization of the thermal properties was done using thermogravimetric analysis (TGA) and differential scanning (DSC). Most of the polymers displayed good film forming properties when cast from NMP solutions. The thermal properties of the polymers were very impressive with glass transition temperatures above 200 °C and 5 % weight loss temperatures of over 470 °C under a nitrogen atmosphere.

## TABLE OF CONTENTS

### 1. INTRODUCTION

1.1 Organic light emitting diode.....	1
1.2 Device structure and fabrication.....	2
1.3 Fluorescent organic materials for OLED.....	4
1.3.1 Small Molecules.....	4
1.3.2 Conjugated polymers.....	5
1.4 Band Gap Energy and Color.....	6
1.5 Solvent Effects on UV and Fluorescence Spectra.....	8
1.6 Poly (arylene ether)s, PAEs.....	9
1.6.1 Poly(arylene ether phosphine oxide), PAEPO.....	9
1.6.2 Polymerization via Nucleophilic Aromatic Substitution (NAS).....	10
1.6.3 Pre and Post modification of polymers.....	11
1.6.4 Poly(arylene ether-benzoxazole), PAEBO and poly(arylene ether-benzothiazole) (PAEBT).....	12
1.6.5 Poly(arylene ether)s with pendent benzoxazole or benzothiazole.....	14
1.7 Current project.....	16

## 2. EXPERIMENTAL

2.1. Instrumentation .....	17
2.2 Materials.....	17
2.3 Synthesis of BOX-Br .....	18
2.4 Synthesis of BOX-CBZ.....	19
2.5 Synthesis of BOX-IND.....	20
2.6 Iodination BTZ .....	21
2.7 Synthesis of BTZ-CBZ monomer.....	22
2.8 Representative synthesis of BOX-CBZ copolymers ( <b>10a-10d</b> ).....	23
2.9 Synthesis of BTZ-CBZ copolymer.....	23
2.10 Synthesis of BOX-IND copolymer.....	24
2.11 Characterization	
2.11.1 Nuclear Magnetic Resonance (NMR) Analysis.....	25
2.11.2 Thermogravimetric Analysis (TGA) .....	25
2.11.3 Differential Scanning Calorimetry (DSC).....	25
2.11.4 Absorption and Emission Spectra .....	26

### **3. RESULTS AND DISCUSSION**

3.1 Synthesis of BOX-BR.....	27
3.2 Synthesis of BOX-CBZ .....	30
3.3 Synthesis of BOX-IND .....	33
3.4 Iodination of BTZ.....	35
3.5 Synthesis of BTZ-CBZ .....	37
3.6 UV and Fluorescence of monomers BOX-CBZ, BOX-IND, BTZ-CBZ.....	40
3.7 Synthesis of copolymers <b>10a-10d</b> , <b>11</b> and <b>12</b> .....	42
4 Thermal Analysis.....	47
5 Absorption and Emission .....	50
<b>4. CONCLUSION.....</b>	<b>54</b>
<b>5. FUTURE WORK. ....</b>	<b>56</b>
<b>6. REFERENCES.....</b>	<b>57</b>

## LIST OF FIGURES

<b>Figure 1.</b> Typical OLED Device Structures.....	3
<b>Figure 2.</b> Structures of small fluorescent molecules.....	4
<b>Figure 3.</b> Examples of conjugated fluorescent polymers.....	5
<b>Figure 4.</b> Illustration of HOMO-LUMO energy gap and color.....	6
<b>Figure 5.</b> Fluorescent molecules containing Donor-Acceptor groups.....	7
<b>Figure 6.</b> Monomers synthesized in the current work.....	16
<b>Figure 7.</b> 300 MHz $^1\text{H}$ ( $\text{CDCl}_3$ ) NMR spectrum of BOX-BR ....	28
<b>Figure 8.</b> 75.5 MHz $^{13}\text{C}$ NMR ( $\text{CDCl}_3$ ) spectrum of BOX-BR. ....	29
<b>Figure 9.</b> 300 MHz $^1\text{H}$ NMR ( $\text{CDCl}_3$ ) spectrum BOX-CBZ .....	31
<b>Figure 10.</b> 75.5 MHz $^{13}\text{C}$ NMR ( $\text{CDCl}_3$ ) spectrum BOX-CBZ .....	32
<b>Figure 11.</b> 300 MHz $^1\text{H}$ NMR ( $\text{CDCl}_3$ ) spectrum of BOX-IND monomer. ....	34
<b>Figure 12.</b> 75.5 MHz $^{13}\text{C}$ NMR ( $\text{CDCl}_3$ ) spectrum of BOX-IND monomer ....	35
<b>Figure 13.</b> 300 MHz $^1\text{H}$ NMR ( $\text{CDCl}_3$ ) spectrum of BTZ-I ...	37
<b>Figure 14.</b> 300 MHz $^1\text{H}$ NMR ( $\text{CDCl}_3$ ) spectrum BTZ-CBZ.....	38
<b>Figure 15.</b> 75.5 MHz $^{13}\text{C}$ NMR ( $\text{CDCl}_3$ ) spectrum of BTZ-CBZ .....	39
<b>Figure 16.</b> (a) Absorption and (b) Fluorescence spectra of BTZ-CBZ, BOX-CBZ and BOX-IND in THF, excited at 310 nm.....	40
<b>Figure 17.</b> An overlay of BTZ-CBZ fluorescence spectra in THF and NMP, excited at 300nm.	41

<b>Figure 18.</b> $^{13}\text{C}$ NMR spectrum <b>10a</b> and <b>10c</b> .....	43
<b>Figure 19.</b> $^{13}\text{C}$ NMR spectrum <b>12</b> .....	45
<b>Figure 20.</b> $^{13}\text{C}$ NMR spectrum of <b>11</b> .....	46
<b>Figure 21.</b> Overlay of TGA traces of the polymers <b>10a-10d</b> , <b>11</b> , and <b>12</b> .....	47
<b>Figure 22.</b> DSC traces of the polymers <b>10a-10d</b> , <b>11</b> and <b>12</b> under nitrogen.....	49
<b>Figure 23.</b> (a) Absorption and (b) Emission spectrums of BOX-CBZ copolymers excited at 310nm.....	50
<b>Figure 24.</b> (a) Fluorescence of <b>10a -10d</b> , <b>11</b> and <b>12</b> in NMP. (b) Fluorescence of monomer <b>9</b> and polymer <b>11</b> excited at 310 nm.....	51
<b>Figure 25.</b> Fluorescence of polymer films containing 15% chromophores, excited at 310 nm.....	52
<b>Figure 26.</b> Fluorescence of BTZ-CBZ copolymer under UV lamp.....	53

## LIST OF SCHEMES

<b>Scheme 1.</b> Synthesis of poly(arylene ether phosphine oxide).....	10
<b>Scheme 2.</b> Mechanism of Nucleophilic Aromatic Substitution reaction (NAS).....	11
<b>Scheme 3.</b> Routes for the introduction of functional groups to polymers.....	12
<b>Scheme 4a.</b> Poly(arylene ether-benzoxazole)s (PAEBO).....	13
<b>Scheme 4b</b> Synthesis of poly(arylene ether benzothiazole)s (PAEBT).....	13
<b>Scheme 5.</b> Synthesis of poly(arylene ether)s with pendent benzoxazole or benzothiazole from from 2,6-difluorinated system .....	14
<b>Scheme 6.</b> Synthesis of poly(arylene ether)s with pendent benzoxazole or benzothiazole from 3,5-difluorinated system .....	15
<b>Scheme 7.</b> Synthesis of BOX-Br. ....	27
<b>Scheme 8.</b> Synthesis of BOX-CBZ monomer .....	30
<b>Scheme 9.</b> Synthesis of BOX-IND monomer. ....	33
<b>Scheme 10.</b> Synthesis of BTZ-I .....	36
<b>Scheme 11.</b> Synthesis of BTZ-CBZ monomer .....	38
<b>Scheme 12.</b> Synthesis of polymers <b>10a-10d, 11, and 12</b> .....	42

## LIST OF TABLES

<b>Table 1.</b> Glass transition ( $T_g$ ) and 5% degradation temperatures for polymers <b>10a-10d</b> , <b>11</b> , and <b>12</b> . .....	48
--	----

## ACKNOWLEDGEMENTS

I would like to express my sincere gratitude to my research advisor, Dr. Eric Fossum for his guidance, patience, and inspiration throughout the program. I have exceedingly benefited from his vast knowledge, encouragement, and exceptional personality. Thank you to my committee members, Dr. William Feld and Dr. Daniel Ketcha. I would also like to thank Dr. Fossum's research group, as well as the faculty and staff members of the Wright State University Department of Chemistry.

I would also like to acknowledge Dr. David Dolson and Dr. Pavel's research groups for their advice and guidance in UV and Fluorescence measurements. Thanks to Dr. Ioana Pavel for allowing us to use their analytical instruments for measurements.

My loving wife, Lenah, deserve a lot of recognition for encouragement and understanding throughout the program. Words cannot express my gratitude for your determination and hard work in bringing up our son, Ethan.

This work was supported by a grant from the National Science Foundation, CHE-1307117.

## **DEDICATION**

Dedicated to my loving wife, Lenah and my son, Ethan

for

their love, support, and encouragement

# 1. INTRODUCTION

## 1.1 Organic light emitting diode

Over the past few years, the lighting and display industry has seen rapid growth and development in technology due to the discovery of new and advanced materials that are highly efficient and easy to fabricate into lighting devices. Among the leading devices currently in the market are the light emitting diodes (LED). LED is a semiconductor device that emits visible light when an electric current passes through it. There are two types of LEDs, the Inorganic Light Emitting Diode (ILED), which utilize some metals to emit light, and the Organic Light Emitting Diodes (OLED) which utilize organic materials to emit light. ILED was first developed in the early 1960s, and have achieved a great success in performance and fluorescence lifetime. The cost of ILED is still high due to processing difficulties and high cost of rare elements used as emitters. Despite the challenges, ILEDs have been used extensively in lighting and displays and have shown better efficiencies compared to incandescent bulbs and fluorescent tubes.

The OLED technology has attracted much attention among scientists due to ease of fabrication of OLED devices, and the possibility of design and synthesis of molecules with different optoelectronic properties. This, together with the high demand for advanced materials for lighting and display devices, has led to numerous research in OLED and rapid growth in the industry. Due to their superior performance, organic emitting materials are currently considered as the next-generation lighting and display technology for many applications and a good alternative to the more expensive ILED. The OLED technology now plays a significant role in flat-panel displays, solid-state lighting, and organic solar cells.

Early OLED devices utilized high voltage, mainly AC current, which was applied to thin films of the organic material.<sup>1</sup> In the 1960's, Pope and his team developed a DC driven OLED device with a single crystal of anthracene as the emitter.<sup>1,2</sup> The device required a voltage too high for ease of operation (>300v) and was not reliable enough to further exploit for commercial purposes.<sup>1,2</sup> Scientists were unable to lower the device driving voltage until the 1980s when the voltage was noticeably reduced, but the efficiency was still too low to exploit for commercial purposes.<sup>1,2</sup>

The Kodak Company made a big contribution to OLED development by introducing a device structure, consisting of indium tin oxide (ITO)/diamine/AlQ<sub>3</sub>/MgAg, which is almost the same as the ones used today.<sup>1</sup> The layers in the device served different purposes, the ITO, which is a transparent conductor, served as the anode layer, the diamine was utilized as the hole transporting layer, AlQ<sub>3</sub> an emitter and electron transporting material, and MgAg as the cathode.<sup>2</sup> In 1990, a team of British scientists developed an electroluminescent device, using poly (*p*-phenylene vinylene).<sup>1,2</sup> This material simultaneously worked as an electric charge bipolar carrier and emitter. The use of PPV in OLED was the beginnings of polymer light emitting diodes (PLED).<sup>1,2</sup>

## 1.2 Device structure and fabrication

Early studies on device structure and fabrication focused on devices based on single crystal emitters. Numerous reports on device efficiency and lifetime have been published which shows that OLEDs based on single crystals are not useful for practical applications, the high voltages, small light-emitting areas, and difficulty of single crystal processing limits their application.<sup>2</sup> an

alternative to the single crystal devices is thin film devices, they are easy to fabricate and are more efficient for practical and commercial application.

Multilayer device structures consist of layers of organic material, which help to improve device efficiency and lifetime. Many structures consist of a transparent indium tin oxide (ITO) anode, an organic hole transporting layer (HTL), organic electron transporting layer (ETL) and a metal cathode usually aluminum or Al:Mg alloy. Bilayer devices can be fabricated as follow; ITO/HTL/ETL (EML)/METAL or ITO/HTL(EML)/ETL/METAL. The HTL helps with injection of holes from the anode (ITO) into the organic material. ETL injects electrons from the metal cathode. A thin EML can also be sandwiched between the HTL and ETL to form a three-layered structure.<sup>2</sup>

Modern devices make use of buffer layers to improve efficiency by lowering the drive voltage and preventing chemical interactions between the layers, which lower the performance and lifetime of the diode.<sup>2</sup> The figure below shows the three typical OLED device structures. From left to right; Double layered structure with an ETL emitter, double layered with an HTL emitter, and a triple layered device structure.

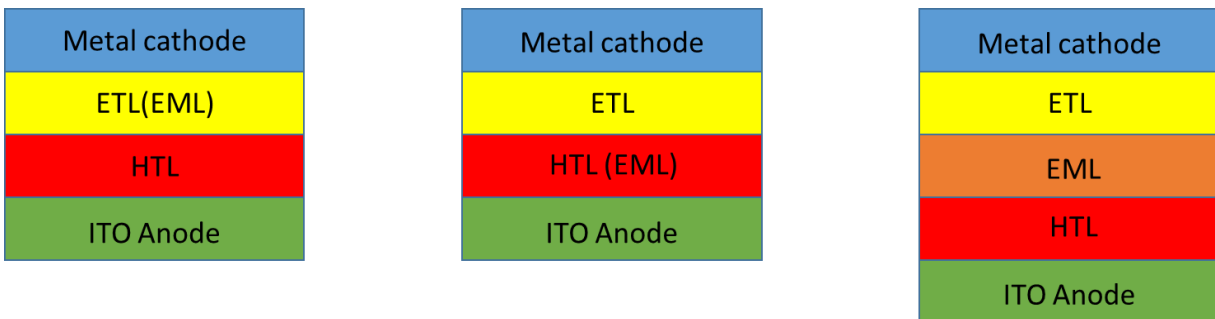


**Figure 1.** Typical OLED Device Structures.

## 1.3 Fluorescent organic materials for OLED

### 1.3.1 Small Molecules

Small molecule OLED technology was pioneered by the Eastman Kodak Company. The technology utilized low molecular weight fluorescent molecules for light emission. Fabrication of a thin layer device is usually done by vacuum or wet deposition which lead to high costs of production and hence limit its use to small-area devices.<sup>2,3</sup> The advantage of the vacuum deposition process is that it enables the formation of uniform films and easy development of very complex structures, which are often more efficient.<sup>2,3</sup> The structures of some small conjugated molecules for OLED applications are shown in **Figure 2**.

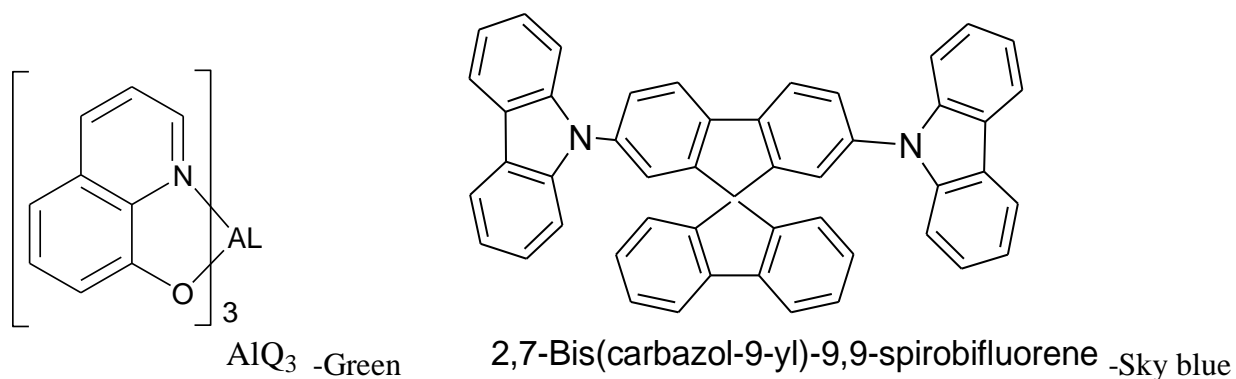


**Figure 2.** Structures of small fluorescent molecules.

**Figure 2** shows two examples of small molecules used for OLED. Tris(8-hydroxyquinolinato)aluminum (AlQ<sub>3</sub>) is a complex in which aluminum is bonded to three 8-hydroxyquinoline ligands. It is one of the earliest and widely investigated fluorescent molecule with good electron transporting properties and green emission. AlQ<sub>3</sub> can be tuned to emit the full light spectrum (RGB) by attaching different electron donating or withdrawing groups to the five

position of the quinolate ligand.<sup>1</sup> 2,7-bis(carbazoyl-9-yl)-9,9-spirobifluorene is a blue emitting small molecule.

### 1.3.2 Conjugated polymers

Conjugated polymers are high molecular weight organic compounds that contain a long chain of alternating single and double bonds. The  $sp^2$ -hybridized carbon atoms are bonded to three other atoms, via sigma bonds, leading to one unpaired electron per carbon atom in a  $p_z$  orbital. The carbon atoms along the polymer chain possess the same hybridization which results in a delocalized  $\pi$  system, this allows charge transfer along the polymer chain. The conjugation allows the polymer to exhibit semiconducting properties.<sup>1, 4, 5</sup> The structures of some conducting polymers are shown in **Figure 3**.

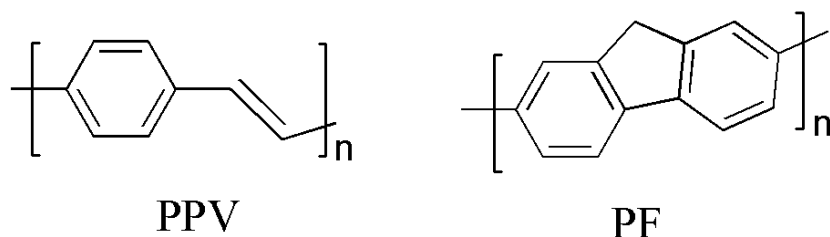


**Figure 3.** Examples of conjugated fluorescent polymers.

Poly(*p*-phenylene vinylene), **PPV**, is the first polymer electroluminescent material to be used for OLED applications. It emits with bright yellow-green color and can be tuned to emit different colors by attaching different organic groups to the polymer backbone. However, due to its poor resistance to light and oxygen degradation, **PPV** is not widely used for OLED applications.

<sup>1 2</sup> Polyfluorene (PF) has attracted considerable attention in the OLED technology due to its high photoluminescence efficiency, high stability, and ability to emit at different wavelengths with some structural modification.

### 1.4 Band Gap Energy and Color

Fluorescent organic molecules contain orbitals that allow movement of electrons from the ground state to the excited state and vice versa. The energy gap ( $E_g$ ) between the highest occupied molecular orbital (HOMO) and the lowest unoccupied molecular orbital (LUMO) determines the wavelength and fluorescence of organic molecules. **Figure 4** illustrates the relationship between  $E_g$  and fluorescence color.

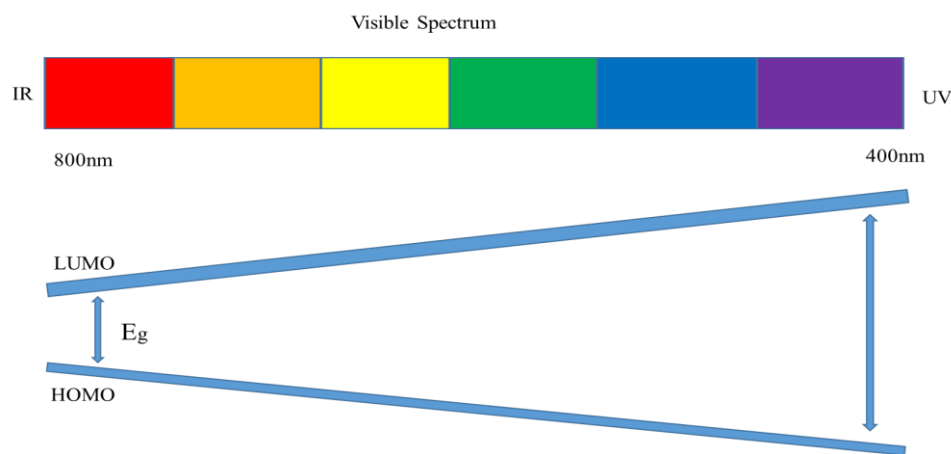


**Figure 4.** Illustration of HOMO-LUMO energy gap and color

Large  $E_g$  values lead to shorter absorption and emission wavelengths, a 'blue shift' and a higher excitation energy, while small  $E_g$  lead to longer absorption and emission wavelengths and a 'red shift'. The energy gap in organic molecules can be tuned to obtain different optoelectronic

properties.<sup>6,7,8</sup> For example, the energy gap in **PPV** can be increased, by reducing the planarization and conjugation between the phenyl and vinyl groups, leading to a blue-shift.<sup>1,7</sup>

Molecules containing an electron-donating group (D) linked to an electron accepting group (A) by  $\pi$ -bonds, D- $\pi$ -A, can be tuned to emit different colors by the appropriate choice of donor or acceptor group. A red shift in emission wavelength of D- $\pi$ -A fluorescent molecules is attributed to the greater charge transfer character caused by higher electron-donating strength or greater electron withdrawing ability and vice versa.<sup>9</sup> The choice of donor and acceptor groups could help to reduce the band gap energy for red emission or increase the band gap energy for blue emission.<sup>1,3,10</sup> **Figure 5** shows an example of a fluorescent molecule containing D- $\pi$ -A. The 2,7-divinyl-9,9-bis(*tert*-butyl)fluorene ( $\pi$ ) forms a  $\pi$ -bridge that connect the electron donor, diphenylamine (D) to an electron acceptor, diphenyloxadiazoled (A), to form a D- $\pi$ -A system. The molecule has strong fluorescence at  $\sim 460$  nm and exhibits good charge transfer properties.<sup>11</sup>

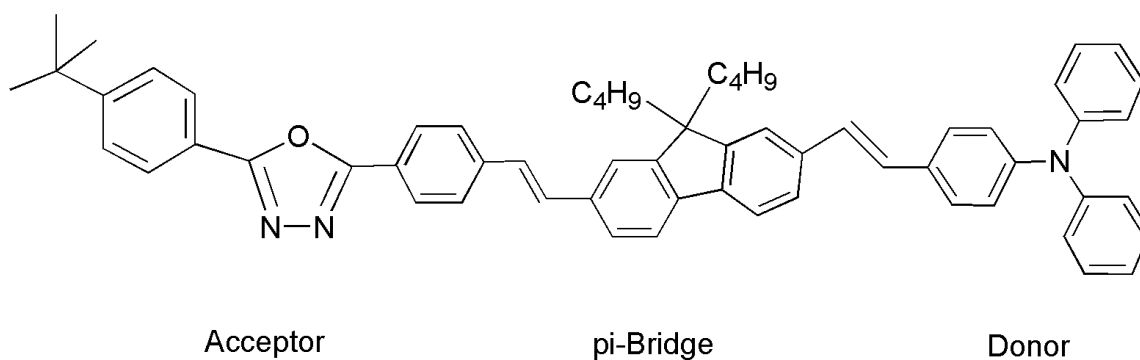


**Figure 5.** Fluorescent molecule containing Donor-Acceptor groups.

## 1.5. Solvent Effects on UV and Fluorescence Spectra

The fluorescence wavelength, intensity, and shape of absorption and emission spectra of organic molecules are usually susceptible to the environment surrounding the fluorescing molecules.<sup>12</sup> Fluorescent molecules in different solvents show spectral shifts which are attributed to interactions between solute and solvent molecules. These interactions can be in the form of hydrogen bonding, acid-base chemistry or bulk solvent effects.<sup>12</sup> The magnitude of the spectral shifts in different solvents depends on the strength of the intermolecular hydrogen bonds between the substituent groups of the chromophore molecule and –OH or –NH groups of the surrounding solvent molecules.<sup>12</sup> Molecules with intramolecular hydrogen system are less affected by solvent polarity due to stronger intermolecular attraction, while systems without intramolecular hydrogen bond are highly affected.

Molecules with  $\pi$ - $\pi^*$  transitions are shifted to longer wavelength when solvent polarity increases.<sup>12</sup> The excited state of a molecule has an increased dipole moment compared to the ground state hence the fluorescence band maxima of excited states are red-shifted significantly more when the solvent polarity increases compared to the absorption band under the same conditions. Conjugated polymers also show unique fluorescence in the solid state, more ordered polymers have redder spectra and lower quantum yield due to strong interactions between molecules which lead to loss of energy in the excited states or quenching, while polymer chains in poorly packed regions behave nearly as if in solution, having bluer spectra, high quantum yields, and exponential decay.<sup>4, 12,</sup>

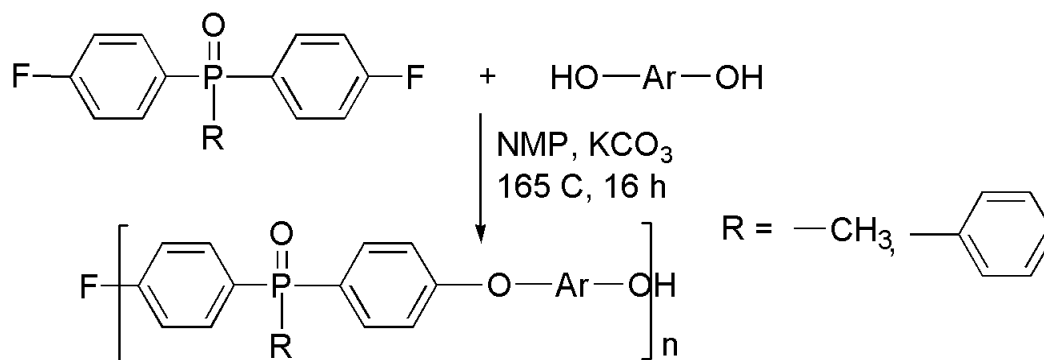
## 1.6 Poly (arylene ether)s, PAEs

Poly(arylene ether)s, **PAE**, are engineering thermoplastics whose structures consist of aromatic rings linked by ether bonds. They have excellent thermal stability and mechanical properties due to the presence of rigid, electron rich aromatic groups in their backbone. They are commonly used in many industrial applications due to their excellent resistance towards hydrolysis and oxidation. Some **PAEs** discussed in this work include poly(phenylene oxide), **PPO**, poly(arylene ether benzoxazole and benzothiazole), poly(arylene ethers) with pendent benzoxazole or benzothiazole units, and poly(arylene ether phosphine oxide), **PAEPO**.

### 1.6.1 Poly(arylene ether phosphine oxide), PAEPO

**PAEPOs** are high performance engineering thermoplastic materials with excellent hydrolytic, thermal and oxidative stability, possessing a glass transition temperature,  $T_g$ , range from 190 °C – 280 °C. They are more self-extinguishing than any other engineering thermoplastics tested when burning, due to the presence of phosphorus.<sup>13, 14</sup> They have high resistance to aggressive oxygen plasma environments, which is achieved by forming a highly oxidized, non-volatile phosphorus-containing surface layer. They are synthesized via nucleophilic aromatic substitution polymerization of bisphenols with phosphorus containing activated dihalides (**Scheme 1**). The reaction is accomplished in the presence of a weak base, potassium carbonate, and a polar aprotic (NMP) at temperature around 175 °C. **PAEPOs** have excellent thermal stability, losing 5% of their weight typically at about 500 °C and a high degree of char at 600 °C-800 °C.<sup>14</sup> As compared to other commercially available engineering thermoplastics like poly(ether ether

ketone), **PEEK**, and bisphenol A polysulfone, **UDEL**<sup>®</sup>, **PAEPOs** shows between 20% and 40% char yield, at high temperatures while **PEEK** and **UDEL**<sup>®</sup> are completely volatilized by 700 °C.<sup>6,15</sup>

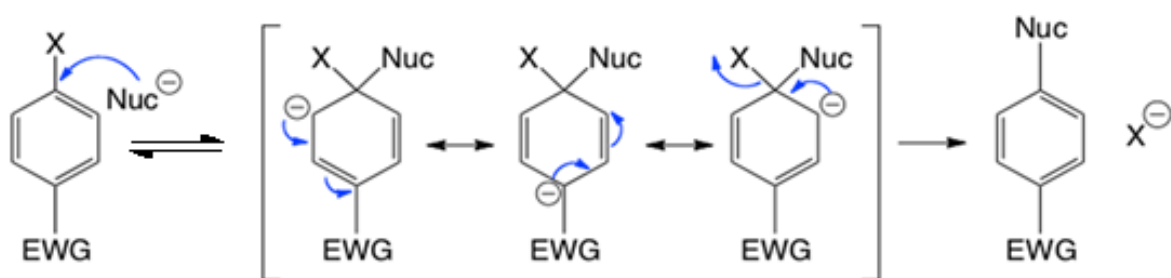


**Scheme 1.** Synthesis of poly(arylene ether phosphine oxide).

### 1.6.2 Polymerization via Nucleophilic Aromatic Substitution (NAS)

Nucleophilic Aromatic Substitution is a reaction in which a nucleophile substitutes a good leaving group (LG), usually a halide on an activated benzene ring. The aromatic ring requires activation by a strong electron-withdrawing group in the *ortho*, *meta*, or *para* positions. The bonding between an electron withdrawing group and *ipso* carbon creates polarization effects due to the unequal distribution of electrons in the sigma bond. The more electronegative atom (EWG) will have a greater pull on the electrons causing a partial negative charge on the more electronegative atom and a partial positive on the *ipso* carbon. As shown in **Scheme 2**, the mechanism involves attack at the electrophile by the nucleophile, forming a resonance-stabilized

anion known as a Meisenheimer complex. This step is slow and hence the rate determining step. The second step occurs when the negative charge on the ring pushes out the leaving group to rearomatize the ring. The second step is fast since the aromaticity of the ring is restored. Electron Donating Groups (EDG) on the other hand deactivate the ring by destabilizing the intermediate formed in the first step of reaction. <sup>17</sup>

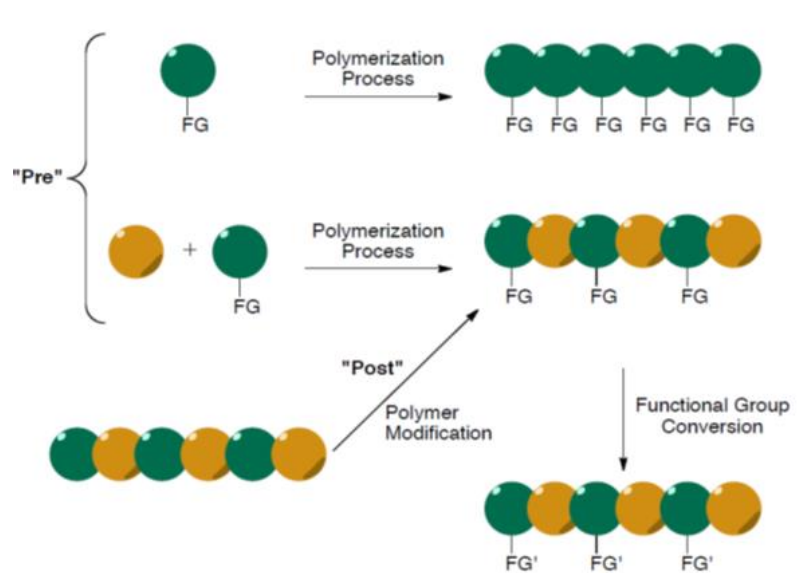


**Scheme 2.** Mechanism of Nucleophilic Aromatic Substitution reaction (NAS).

### 1.6.3 “Pre” and “Post” Modification

Functional groups can be introduced into polymers to obtain desired physical and chemical properties (**Scheme 3**). This can be done in two ways. First is pre-functionalization in which the monomer units are modified before polymerizing. The monomers are then polymerized to give a functionalized polymer. Functionalized monomers can also be copolymerized with unmodified monomers to form copolymers with desired properties. The second method involves introducing functional groups at the polymer stage, also known as post modification. Pre-functionalization requires that the functional groups introduced into the monomer remain unaffected by the

polymerization conditions. The post modification on the other hand is limited by the difficulty in controlling the location of functional groups.

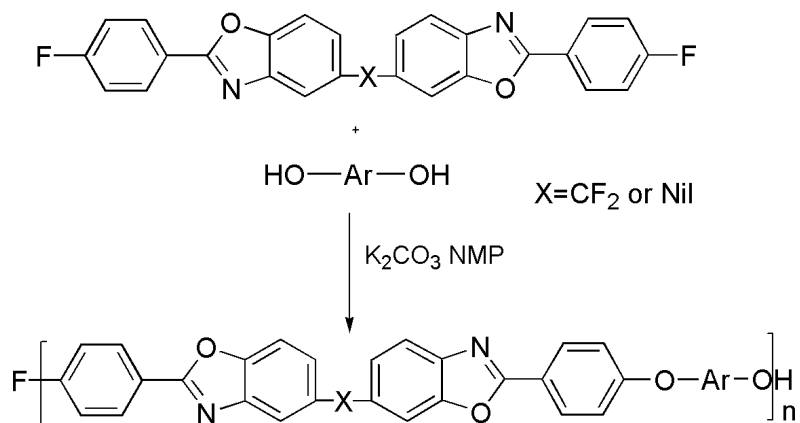


**Scheme 3.** Routes for the introduction of functional groups to polymers.

#### 1.6.4 Poly(arylene ether-benzoxazole), PAEBO and poly(arylene ether-benzothiazole) (PAEBT)

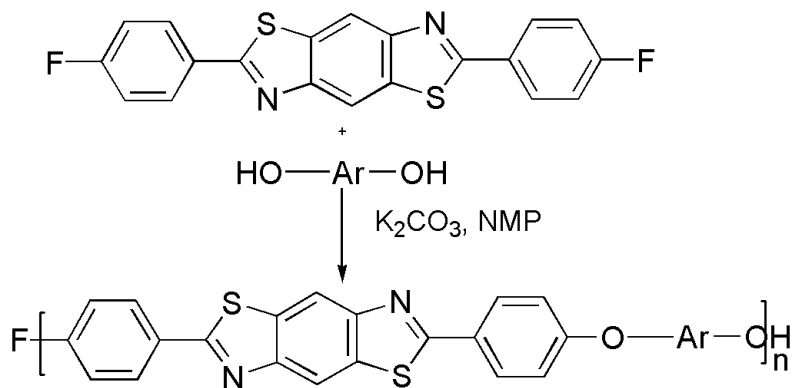
Poly(arylene ether-benzoxazole), **PAEBO**, can be prepared by nucleophilic aromatic substitution (**Schemes 4a**). Fluorine atoms in the *para*-substituted bisbenzoxazoles are activated towards NAS and are readily displaced by phenoxides. Different bisphenols can be used to synthesize the polymers in the presence of NMP solvent and  $K_2CO_3$ . The polymerization process is accomplished by formation of aryl-ether bonds. The polymers can be processed from solutions or melt due to their thermal stability. **PAEBOs** show high  $T_g$  values, ranging from 213 °C to 300

°C, and decomposition temperatures of over 450 °C. The structure of the polymers can easily be modified by using different bisphenols in the polymerization reaction.<sup>18, 19</sup>



**Scheme 4a.** Poly(arylene ether-benzoxazole)s, **PAEBO**

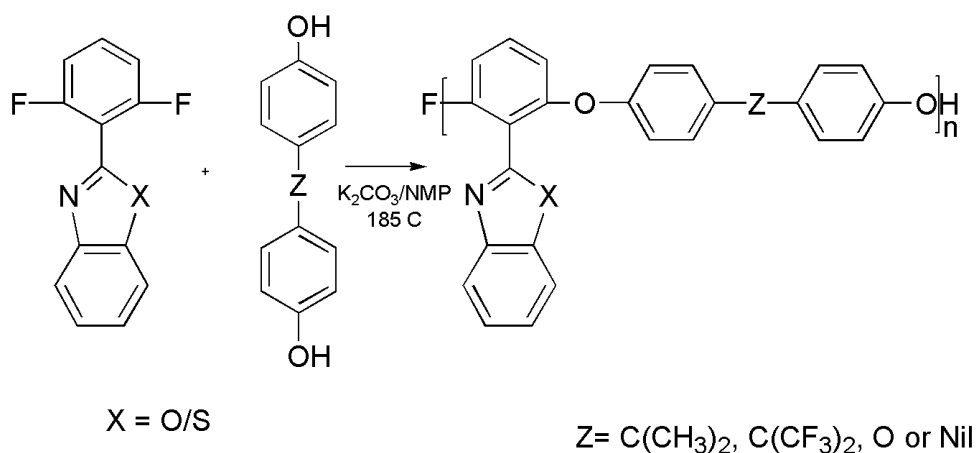
Like poly(aryl benzoxazole)s, poly(arylene ether benzothiazole)s, **PAEBT**, can be synthesized via nucleophilic aromatic substitution (**Scheme 4b**). The benzothiazole heterocycle activates an aromatic halogen group for the displacement reaction with phenoxides. The polymers have high glass transition temperature and degradation temperature of over 450 °C.<sup>19</sup>



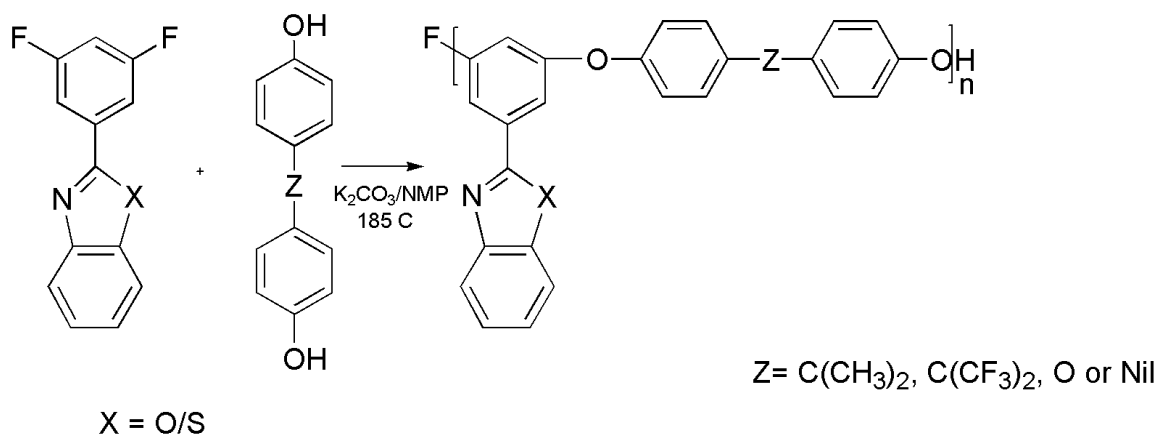
**Scheme 4b.** Synthesis of poly(arylene ether benzothiazole)s, **PAEBT**.

### 1.6.5 Poly(arylene ether)s with pendent benzoxazole or benzothiazole (PAE-pBO and PAE-pBT)

Like PAEPO, PAE-pBO and PAE-pBT are high performance engineering thermoplastics. They have high glass transition temperatures, high thermal stability, and good mechanical properties. Synthesis of PAE-pBO and PAE-pBT is done via typical nucleophilic aromatic substitution of dihalogenated aromatic group which are activated towards NAS by a strong electron withdrawing group with bisphenols. The reaction occurs at 185 °C in a polar aprotic solvent. Monomers containing 2,6 difluorinated systems, 2-(2,6-difluorophenyl)benzoxazole, and 2-(2,6-difluorophenyl)-benzothiazole, were synthesized by J. Hedrick and coworkers. They successfully copolymerized with bisphenol-A, yielding high molecular weight polymers with pendent benzoxazole or benzothiazole **Scheme 5**.<sup>20</sup> PAE-pBO and PAE-pBT have also been synthesized using 3,5 difluorinated systems to form high molecular weight polymers with impressive properties, **Scheme 6**.<sup>17, 20</sup>



**Scheme 5.** Synthesis of poly(arylene ether)s with pendent benzoxazole or benzothiazole groups from 2,6-difluorinated system.



**Scheme 6.** Synthesis of poly(arylene ether)s with pendent benzoxazole or benzothiazole groups from 3,5 difluorinated system.

## 1.7 Current project

The current project seeks to design and synthesize PAE-based fluorescent polymers, in which the backbone is not a conjugated polymer, for blue organic light emitting diodes (OLED). Two difluorinated monomers, which are activated toward NAS reactions by either a benzothiazole or benzoxazole group located in the *meta*-positions (**Figure 6**), are prepared for use in the polymerization reaction. The goal is to utilize the benzoxazole and benzothiazole as acceptor groups for donor/acceptor chromophores. Donor groups, which are electron rich aromatic amines, are attached to the acceptor to form a 'Push-Pull' system, which allows charge transfer between the donor and acceptor. The properties of PAEs, which include high resistance to hydrolysis, thermal stability, and strong resistance to oxidation, can allow for better device performance in extreme conditions of heat and air.

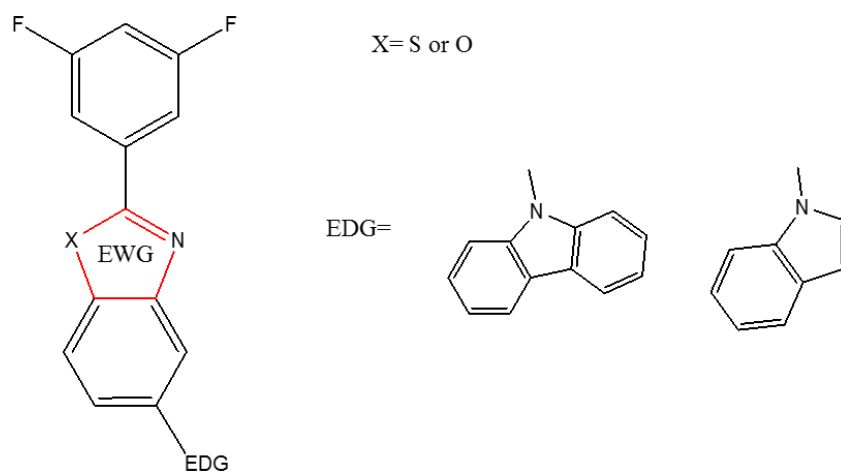


**Figure 6.** Monomers containing electron donating group, EDG, and electron withdrawing group, EWG, used in polymer synthesis.

## 2. EXPERIMENTAL

### 2.1 Instrumentation

A Bruker AVANCE 300 MHz instrument was used to acquire  $^1\text{H}$  and  $^{13}\text{C}$  Nuclear Magnetic Resonance (NMR) spectra. The instrument operates at 300 and 75.5 MHz, for  $^1\text{H}$  and  $^{13}\text{C}$ , respectively. Monomer samples were dissolved in an appropriate deuterated solvent (DMSO- $d_6$  or  $\text{CDCl}_3$ ) at a concentration of  $\sim 35\text{mg} / 0.7\text{ mL}$ , while polymer samples were dissolved in a NMP-DMSO- $d_6$  mixture (40 mg / 0.2:0.5 mL). A Hewlett-Packard (HP) 6890 Series GC, coupled with a HP 5973 Mass Selective Detector/Quadrupole system, was used to perform GC/MS analyses. Differential Scanning Calorimetry (DSC) and Thermogravimetric analyses (TGA) were carried out on TA Instruments DSC Q200 (under nitrogen) and TGA Q500 (under nitrogen or air), respectively, at a heating rate of  $10\text{ }^\circ\text{C} / \text{min}$ . Melting points were determined on a MEL-TEMP instrument and elemental analyses were obtained from Midwest Micro Labs Inc., Indianapolis, IN. Fluorescence data was acquired using an Agilent Technologies Cary Eclipse fluorescence Spectrophotometer, while UV/Vis data was acquired using an Agilent Cary 60 UV-VIS Spectrometer.

### 2.2 Materials

The compounds 2-Amino-4-bromophenol and 3,5-difluorobenzoic acid were purchased from Oakwood Chemicals and used as received. *N*-Iodosuccinimide was purchased from Oakwood Chemicals and used as received. 2-Aminothiophenol and *N,N*-dimethylglycine were purchased from Sigma Aldrich and used as received. Carbazole was purchased from Sigma Aldrich and recrystallized from chloroform before use. Indole was purchased from Lancaster Labs and used as

received. 4,4'-Biphenol was purchased from TCI and recrystallized from hexanes with a few drops of ethanol. *Bis*-(4-fluorophenyl)phenylphosphine oxide was received from Daychem Laboratories. Copper (I) iodide was purchased from Sigma Aldrich and activated by washing in a Soxhlet extractor with hot THF. Potassium carbonate was purchased from Sigma Aldrich and dried at 130 °C in oven. Calcium carbonate was purchased from Allied Chemicals and dried in oven at 130 °C before use. Sodium bicarbonate was purchased from Fisher Chemicals. NMR solvents, Chloroform-*d* (CDCl<sub>3</sub>) and dimethyl sulfoxide-*d*<sub>6</sub> (DMSO-*d*<sub>6</sub>) were purchased from Sigma Aldrich. *N*-Methylpyrrolidinone (NMP) was purchased from Sigma Aldrich dried over CaH<sub>2</sub> and distilled under nitrogen prior to use. 2-(3,5-difluorophenyl)-benzothiazole (**BTZ**) was synthesized via a previously reported route. Tetrahydrofuran (THF) was received from Macron. Dimethyl sulfoxide (DMSO) was received from Sigma Aldrich, dried over CaH<sub>2</sub> and distilled under nitrogen before use. Chloroform (CHCl<sub>3</sub>) and sulfuric acid (H<sub>2</sub>SO<sub>4</sub>) were purchased from BDH. Toluene was purchased from EMA and used as received. Ethanol was received from Decon Labs Inc. Non-iodized Morton salt was purchased from a local Meijer store and used as received.

### 2.3 Synthesis of BOX-Br, 3

In a 250 mL round-bottomed (RB) flask, equipped with a stir bar and condenser, were placed 2-amino-4-bromophenol (5.0 g, 26 mmol), 3,5-difluorobenzoic acid (5.5 g, 32 mmol) and 50 g of polyphosphoric acid (PPA). The mixture was immersed in a silicone oil bath and heated to 90 °C for 12 h and subsequently to 130 °C for 12 h. An aliquot was removed and analyzed via GC/MS, which showed ~ 100% conversion. The reaction mixture was slowly poured into 500 mL of vigorously stirred DI water, and the resulting brown solid was isolated by filtration. The solid

was dissolved in toluene (200 mL) and washed with DI water (3 X 400 mL), 5% NaHCO<sub>3</sub> (2 X 50 mL), DI water (300 mL) and finally with brine (100 mL). The toluene layer was dried over magnesium sulfate, filtered and the solvent was removed via rotary evaporation. The resulting pink solid was recrystallized from ethanol/water, isolated by vacuum filtration and dried under vacuum to afford 8.16 g (98.0 %) of **3** as light pink crystals with a melting point of 178-179 °C. <sup>1</sup>H NMR (CDCl<sub>3</sub>; δ): 7.01 (tt, <sup>3</sup>J<sub>F-H</sub> = 8.6, <sup>4</sup>J<sub>H-H</sub> = 2.4, 1H), 7.46 (dd, <sup>3</sup>J<sub>H-H</sub> = 8.7, <sup>5</sup>J<sub>H-H</sub> = 0.6, 1H), 7.51 (dd, <sup>3</sup>J<sub>H-H</sub> = 8.6, <sup>4</sup>J = 1.9, 1H), 7.75 (m, 2H), 7.91 (dd, <sup>4</sup>J<sub>H-H</sub> = 1.8, <sup>5</sup>J<sub>H-H</sub> = 0.6, 1H) <sup>13</sup>C NMR (CDCl<sub>3</sub>; δ): 107.2, 110.7, 112.0, 117.8, 123.4, 128.9, 129.5, 143.3, 149.7, 161.7, 163.9.

#### 2.4 Synthesis of benzoxazole–carbazole monomer (BOX-CBZ), **5a**

To a 250 mL RB flask, equipped with stir bar and condenser, were added 2-(3,5-difluorophenyl) 5-bromobenzoxazole (5.0 grams, 16 mmol), carbazole (7.0 g, 41 mmol), K<sub>2</sub>CO<sub>3</sub> (5.0 g), CuI (10 mol %), *N,N*-dimethylglycine (20 mol %) and DMSO (6 mL). The mixture was heated to 80°C in an oil bath for 52 h. Analysis of an aliquot showed 100% conversion. The reaction mixture was cooled to room temperature and precipitated from vigorously stirred DI water (500 mL). The greenish precipitate was separated by vacuum filtration and dissolved in chloroform. The solution was washed with DI water (2 x 500 mL). The organic layer was separated from the aqueous layer and 200 mL of ethanol were added to the organic layer. The chloroform was removed by house vacuum (~ 100 torr), which allowed the product, **BOX-CBZ** to crystallize, leaving residual carbazole in solution. The crystals were isolated by vacuum filtration and the resulting solid was recrystallized from a chloroform–ethanol mixture (1:3) to afford 5.61 g (87%)

of light pink, **BOX-CBZ** crystals with a melting point of 213-214°C. Elemental analysis, Theoretical; C=75.51%, H=3.54%. Found; C=75.48, H=3.58. <sup>1</sup>H NMR (CDCl<sub>3</sub>; δ): 7.06 (tt, <sup>3</sup>J<sub>H-F</sub> = 8.6, <sup>4</sup>J<sub>H-H</sub> = 2.4, 1H), 7.34 (ddd, <sup>3</sup>J<sub>H-H</sub> = 7.7, <sup>3</sup>J<sub>H-H</sub> = 6.1, <sup>4</sup>J<sub>H-H</sub> = 2.1, 2H), 7.48-7.40 (m, 4H), 7.62 (dd, <sup>3</sup>J<sub>H-H</sub> = 8.6, <sup>4</sup>J<sub>H-H</sub> = 2.1, 1H), 7.83 (dd, <sup>3</sup>J<sub>H-H</sub> = 8.6, <sup>5</sup>J<sub>H-H</sub> = 0.4, 1H), 7.86 (m, 2H), 8.02 (dd, <sup>4</sup>J<sub>H-H</sub> = 2.1, <sup>5</sup>J<sub>H-H</sub> = 0.6, 1H), 8.20 (m, 2H) <sup>13</sup>C NMR (CDCl<sub>3</sub>; δ): 107.3, 109.6, 110.8, 111.9, 119.4, 120.1, 120.4, 123.4, 125.4, 126.08, 129.7, 134.9, 141.2, 143.1, 149.8, 151.5, 162.2, 163.3

## 2.5 Synthesis of benzoxazole-indole monomer (BOX-IND), 5b

A 10 mL RBF, equipped with a stir bar and condenser was charged with **BOX-Br** (2.0 g, 6.5 mmol), indole (3.0 g, 18 mmol), *N,N*-dimethylglycine (20 mole %) CuI (10 mole %), K<sub>2</sub>CO<sub>3</sub> (18mmol) and DMSO (4 mL). The reaction was allowed to proceed at 80 °C for 24 h, at which point GC-MS analysis showed ~100 % conversion. The sample was precipitated from water (500 mL) and extracted into 200 mL of chloroform. The organic layer was separated and washed with DI water (2 X 300 mL), 5% HCL solution (100 mL) and finally two times with DI water (2 X 400 mL). The solvent was removed and the resulting solid was triturated in warm (55 °C) water to remove excess indole. The trituration mixture was filtered and the resulting brown solid recrystallized from 70 mL ethanol to afford 1.9 g (85%) of white-brown crystals of **BOX-IND** with a melting point of 130-132 °C. Elemental analysis; Theoretical C=72.73, H=3.49. Found C=72.37, H=3.61. <sup>1</sup>H NMR (CDCl<sub>3</sub>; δ): 6.76 (dd, <sup>3</sup>J<sub>H-H</sub> = 3.2, <sup>4</sup>J<sub>H-H</sub> = 0.6, 1H), 7.05 (tt, <sup>3</sup>J<sub>F-H</sub> = 8.6, <sup>4</sup>J<sub>H-H</sub> = 2.3, 1H), 7.22 (m, 1H), 7.31-7.26 (m, 1H), 7.41 (d, <sup>3</sup>J<sub>H-H</sub> = 3.3, 1H), 7.57 (dd, <sup>3</sup>J<sub>H-H</sub> = 6.9, <sup>4</sup>J<sub>H-H</sub> = 1.7, 1H), 7.60 (d, <sup>3</sup>J<sub>H-H</sub> = 4.4, 1H), 7.73 (d, <sup>3</sup>J<sub>H-H</sub> = 2.5, 1H), 7.75 (d, <sup>2</sup>J<sub>H-H</sub> = 6.1, 1H), 7.86-7.82 (m, 2H), 7.94 (d, <sup>4</sup>J<sub>H-H</sub> = 1.9, 1H). <sup>13</sup>C NMR (CDCl<sub>3</sub>; δ): 103.9, 107.2, 110.8, 116.4, 120.5, 121.2, 122.6, 122.9, 128.8, 129.2, 129.7, 136.2, 137.2, 142.8, 149.2, 162.2, 163.3

## 2.6 Iodination of 2-(3,5-Difluorophenyl)-benzothiazole, (BTZ)

2-(3,5-Difluorophenyl)-benzothiazole (**BTZ**) was prepared by the reaction of 2-amino thiophenol with 3,5-difluorobenzoic acid in polyphosphoric acid.<sup>21, 22</sup> For iodination of **BTZ**, a RBF equipped with a stir bar and a gas outlet was charged with 2-(3,5 difluorophenyl)-benzothiazole (2.0 g, 8.0 mmol), *N*-iodosuccinimide (1.96 g, 8.00 mmol) and H<sub>2</sub>SO<sub>4</sub> (10 mL). The reaction was allowed to proceed at room temperature for 24 h. An aliquot from the reaction mixture showed 87 % **BTZ-I**, **8a**. The mixture was precipitated from DI water (500 mL) and filtered by vacuum filtration. The pink solid was dissolved in toluene, washed with 5% sodium carbonate solution (100 mL) followed by DI water (2 X 200 mL). The mixture was separated via separatory funnel and dried in a rotary evaporator, The purple solid was dissolved in chloroform (200 mL) and decolorized by vigorously stirring in a solution of 10 % sodium bisulfite (100 mL) for 10 min. The mixture was washed with DI water (2 X 200 mL) and brine (200 mL) and separated via separatory funnel, followed by removing the solvents via rotary evaporation. The resulting solid was recrystallized from a mixture of chloroform, ethanol and toluene (1:1:8) to afford white crystals of **BTZ-I** (1.53 g, 52%) with a melting point of 148-149°C. <sup>1</sup>H NMR (CDCl<sub>3</sub>; δ): 6.96 (tt, <sup>3</sup>J<sub>H-F</sub> = 8.6, <sup>4</sup>J<sub>H-H</sub> = 2.4, 1H), 7.61 (m, 2H), 7.80 (s, 1H), 7.81 (s, 1H), 8.26 (s, 1H)

## 2.7 Synthesis of BTZ-CBZ, 9

To a 10 mL round bottomed flask, equipped with a magnetic stir bar and condenser, were added BTZ-I (0.50 g, 1.3 mmol), carbazole (0.70 g, 4.0 mmol), CuI (10 mole %), dimethylglycine (20 mole %), K<sub>2</sub>CO<sub>3</sub> (0.5 g, 4 mmol) and DMSO (3 mL). The reaction mixture was placed in an oil bath and heated to 80°C for 24 h at which point an aliquot was taken for GC-MS analysis, which showed ~100% conversion. The entire reaction mixture was then precipitated from 500 mL of vigorously stirred water and the resulting solid isolated via vacuum filtration. The resulting greenish solid was dissolved in chloroform (150 mL), washed with DI water (2 X 300 mL) and separated via a separatory funnel. Ethanol was added to the mixture and the chloroform was removed by applying house vacuum (~ 100 torr) in a closed side arm flask for 6 h. The resulting solid was isolated via filtration and recrystallized from a 20% ethanol-chloroform mixture. The crystals were separated by filtration, rinsed with ethanol and dried to afford 0.4 g (78%) of **BTZ-CBZ** as white crystals. <sup>1</sup>H NMR (CDCl<sub>3</sub>; δ): 7.01 (tt, <sup>3</sup>J<sub>H-F</sub> = 8.6, <sup>4</sup>J<sub>H-H</sub> = 2.3, 1H), 7.35 (ddd, <sup>3</sup>J<sub>H-H</sub> = 7.9, <sup>3</sup>J<sub>H-H</sub> = 4.6, <sup>4</sup>J<sub>H-H</sub> = 3.4, 2H), 7.47-7.45 (m, 4H), 7.71-7.68 (m, 2H), 7.75 (dd, <sup>3</sup>J<sub>H-H</sub> = 8.7, <sup>4</sup>J<sub>H-H</sub> = 2.1, 1H), 8.12 (dd, <sup>4</sup>J<sub>H-H</sub> = 2.1, <sup>5</sup>J<sub>H-H</sub> = 0.5, 1H), 8.19 (M, 2H), 8.31 (dd, <sup>3</sup>J<sub>H-H</sub> = 8.7, <sup>5</sup>J<sub>H-H</sub> = 0.5, 1H) <sup>13</sup>C NMR (CDCl<sub>3</sub>; δ): 106.4, 109.7, 110.5, 120.1, 120.3, 120.4, 123.6, 124.8, 126.1, 126.2, 135.6, 136.3, 136.4, 140.9, 152.8, 163.2, 166.1

## 2.8 Representative synthesis of BOX-CBZ copolymers, 10a-10d

To a 5 mL RBF, equipped with a condenser, magnetic stir bar and nitrogen gas inlet, were added **BOX-CBZ** (0.40 g, 1.0 mmol), bis-(4-fluorophenyl)phenylphosphine oxide (0.95 g, 3.0 mmol), 4,4'-biphenol (0.75 g, 4.0 mmol),  $K_2CO_3$  (0.9 g, 5 mmol),  $CaCO_3$  (0.4 g, 4 mmol) and NMP (6 mL). The reaction mixture was heated to 185°C for 21 h, at which point it was cooled to room temperature, diluted with 2 mL of NMP and then added drop-wise to 400 mL of vigorously stirred acidified (pH ~5) DI water. The resulting precipitate was isolated via vacuum filtration and re-precipitated by first dissolving in NMP (3 mL) and adding drop-wise into 400 mL of vigorously stirred water. The resulting precipitate was filtered followed by air drying on the filter paper and afterwards in a drying pistol to afford 1.58 g (82% yield).

The other two copolymers, 15% and 5% **BOX-CBZ**, bis(4-fluorophenyl)phenylphosphine oxide and biphenol copolymers were synthesized using the same method, only with different ratios of the reactants. The  $^{13}C$  NMR spectra showed similar spectra but with different intensities.

$^{13}C$  NMR (DMSO;  $\delta$ ): 109.9, 115.9, 116.1, 117.8, 118.1, 120.0, 120.6, 122.9, 123.1, 126.3, 126.7, 127.3, 127.9, 128.1, 128.7, 128.9, 130.4, 131.9, 132.4, 132.9, 134.3, 136.1, 137.3, 140.9, 154.2, 155.1, 155.9, 156.8, 157.7, 160.6, 160.9.

## 2.9 Synthesis of BTZ-CBZ copolymer, 11

A 5 mL round bottomed flask, equipped with a stir bar, a condenser and a nitrogen gas inlet was charged with **BTZ-CBZ** (0.09 g, 0.22 mmol), bis(4-fluorophenyl)phenylphosphine oxide (0.39 g, 1.23 mmol), 4,4'-biphenol (0.27 g, 1.45 mmol),  $K_2CO_3$  (0.38 g, 2.90 mmol),  $CaCO_3$  (0.20 g, 0.20 mmol) and NMP (2.4 mL). The reaction was heated in silicon oil bath at 185 °C for 21 h.

The reaction mixture was cooled to room temperature and precipitated from vigorously stirred acidified DI water (400 mL, PH 5) with the resulting solid being isolated via vacuum filtration. The solid was dissolved in NMP (3 mL), precipitated from vigorously stirred DI water (400 mL) and filtered. The solid was air dried on filter paper for 2 h and subsequently in a drying piston for 48 h to afford 0.59 g (85% yield).  $^{13}\text{C}$  NMR (DMSO;  $\delta$ ): 109.9, 111.4, 116.0, 118.20, 118.6, 120.3, 120.6, 120.7, 123.3, 126.6, 126.8, 128.8, 128.7, 128.9, 131.8, 132.2, 133.0, 134.3, 134.4, 134.9, 136.1, 136.5, 140.7, 151.5, 152.9, 155.1, 155.5, 159.6, 160.6

## 2.10 Synthesis of BOX-IND copolymer, 12

To a 5 mL round bottomed flask (RBF), equipped with condenser, magnetic stir bar and nitrogen gas inlet were placed **BOX-IND** (0.100 g, 0.290 mmol), bis(4-fluorophenyl)phenylphosphine oxide (0.510 g, 1.64 mmol), 4,4'-biphenol (0.360 g, 1.92 mmol),  $\text{K}_2\text{CO}_3$  (0.69 g, 5.0 mmol),  $\text{CaCO}_3$  (0.50 g, 5.0 mmol) and NMP (3.2 mL). The flask was immersed in a silicon oil bath and heated at 185 °C for 21 h. The reaction mixture was cooled to room temperature and diluted with NMP (2 mL) and added drop wise into vigorously stirred acidified DI water. The resulting solid was filtered and air dried on the filter paper for two hours. The solid was dissolved in NMP (3 mL) and precipitated from DI water (400 mL), filtered and air dried overnight. The polymer was finally dried in a drying piston for 48 h to afford 0.68 g (76% yield).  $^{13}\text{C}$  NMR (DMSO;  $\delta$ ): 110.5, 110.8, 112.0, 115.9, 116.1, 117.8, 118.1, 120.6, 126.4, 126.7, 127.3, 127.9, 128.1, 128.7, 129.1, 130.4, 131.9, 132.3, 132.9, 134.3, 136.1, 137.3, 138.2, 143.3, 154.1, 155.1, 155.9, 156.8, 157.7, 160.6, 160.9

## **2.11 Characterization**

### **2.11.1 Nuclear Magnetic Resonance (NMR) Analysis**

The NMR spectra were acquired using a Bruker AVANCE 300 MHz Instrument. Due to solubility problems in DMSO, the polymer samples (40 mg) were dissolved in a mixture of NMP and DMSO-*d*<sub>6</sub> (0.2:0.4 mL). <sup>13</sup>C NMR data was acquired overnight, 12 h (12,288 scans), while DEPT-90 <sup>13</sup>C NMR data was acquired for 4 h (4,096 scans).

### **2.11.2 Thermogravimetric Analysis (TGA)**

The thermal stability of the polymers under nitrogen and air was investigated using a TA Instruments Q500 Thermogravimetric Analyzer. The method used involved heating ~6 mg of sample at a rate of 10°C/min from 40°C to 800°C, under a nitrogen or an air atmosphere. The weight loss was recorded as a function of time and the thermal stability was reported as 5% weight loss.

### **2.11.3 Differential Scanning Calorimetry (DSC)**

A TA Instruments, Q200 Differential Scanning Calorimeter was used to investigate any thermal transitions of the polymers. The sample was placed in a Tzero aluminum pan and analyzed using a method that involved heating at 10 °C/min from 40 °C to 250 °C and cooling at 20 °C/min to 40 °C in two cycles under a nitrogen atmosphere. The first heating cycle was utilized to erase the thermal history of the polymers while the glass transition temperatures, T<sub>g</sub>, was determined by finding the midpoint of the tangent of the change in baseline of the second heating cycle.

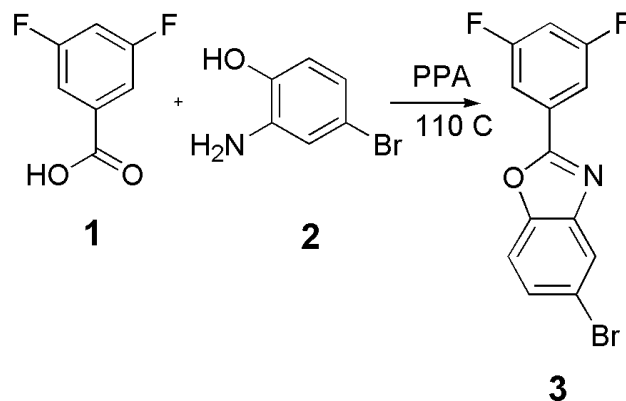
#### **2.11.4 Absorption and Emission Spectra**

The absorption and fluorescence spectra of monomers were first acquired from 5 millimolar solutions in THF and NMP. The absorption and fluorescence data for the monomers were also acquired in both NMP and THF solvents at a concentration of 20 micromolar. Absorption and emission for the polymers were acquired from NMP solutions, at a concentration of 20 micromolar, as well as in film form. The fluorescence of polymer films was measured by placing the films at a 45° angle to the incident light in the fluorescence spectrometer.

### 3. RESULTS AND DISCUSSION

#### 3.1 Synthesis of BOX-Br, **3**

The synthesis of BOX-Br, **3**, was achieved by the reaction of 3,5-difluorobenzoic acid, **1**, with 2-amino-4-bromophenol, **2**, in the presence of polyphosphoric acid, PPA, (**Scheme 7**).<sup>21, 22, 23</sup> The method was previously used and described in the literature by Kashiyama *et al.* and also used by Huong Hoang for the synthesis of 2-(3,5-difluorophenyl) benzothiazole and benzoxazole.<sup>21, 22, 23</sup> The structure of **3** is shown in Scheme 7; in this work, the 3,5-difluorophenyl unit is considered to be the “upper ring”.



**Scheme 7.** Synthesis of BOX-Br, **3**

An excess of **1** was first mixed with polyphosphoric acid and heated at 110 °C with stirring until it formed a uniform mixture. Compound **2** was added into the reaction mixture and allowed to react for 24 h. After the reaction was complete, polyphosphoric acid and excess 3,5-difluorobenzoic acid were removed by precipitating the reaction mixture in excess water. The product was recrystallized from ethanol to afford white crystals of **3** (98 % yield). The structure of **3** was confirmed by <sup>1</sup>H and <sup>13</sup>C NMR spectroscopy; the spectra are shown in Figures **7** and **8**, respectively.

In the  $^1\text{H}$  NMR spectrum of **3** (Figure 7) the peak labelled **a**, at 7.01 ppm, is a triplet of triplets, and is assigned to the proton on the upper phenyl ring between the two fluorine atoms. The triplet of triplets is due to the coupling with the two chemically equivalent fluorine atoms ( $^3J_{\text{H-F}} = 8.6$  Hz) and the two protons in the *meta*-positions, with equal coupling constants ( $^4J_{\text{H-H}} = 2.4$  Hz). The signal from proton labelled **e** appears at 7.46 ppm and is a doublet of doublets due to *ortho*-coupling, with **d** ( $^3J_{\text{H-H}} = 8.7$  Hz), and *para*-coupling, with proton **c** ( $^5J_{\text{H-H}} = 0.6$  Hz). The signal at 7.51 ppm is assigned to proton **d**; this is also a doublet of doublets due to *ortho*-coupling, with **e** ( $^3J_{\text{H-H}} = 8.6$  Hz), and *meta*-coupling with **c** ( $^4J_{\text{H-H}} = 1.8$  Hz). The signal assigned to proton **b** is a multiplet due to coupling with the two non-equivalent fluorines and with proton **a**. The peak at 7.91 ppm is a doublet of doublets and is assigned to **c**, the doublet of doublets is due to *meta*-coupling, with **d** ( $^4J_{\text{H-H}} = 1.8$  Hz), and *para*-coupling, with **e** ( $^5J_{\text{H-H}} = 0.6$  Hz).

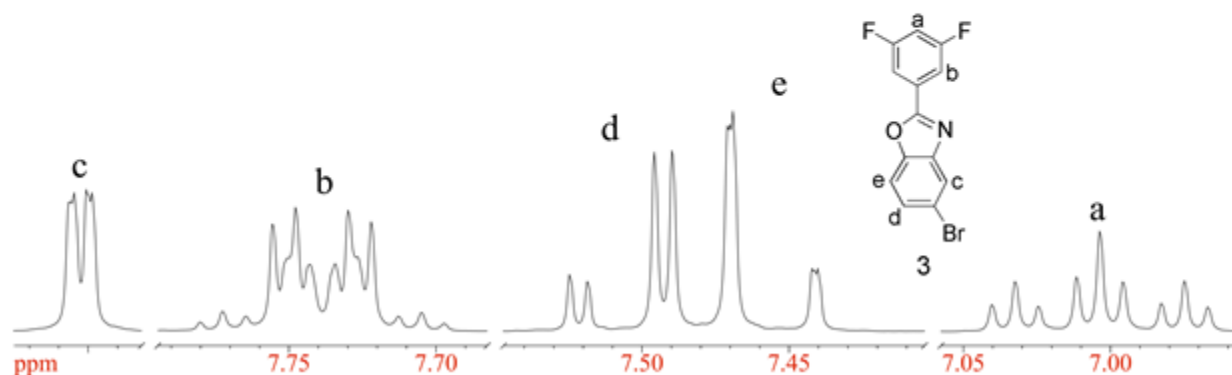


**Figure 7.** 300 MHz  $^1\text{H}$  ( $\text{CDCl}_3$ ) NMR spectrum of **BOX-Br, 3**.

The  $^{13}\text{C}$  NMR spectrum of **3** is shown **Figure 8** and shows eleven unique peaks. The carbon atoms assigned to **a**, **d** and **e**, appearing at 107.2, 129.5 and 163.4 ppm, respectively are all triplets due to coupling with the two fluorine atoms. The signal for carbon **a** is the most upfield due to resonance contributions from the two *ortho* fluorines, which increase electron density. Carbon **b** appears as a doublet of doublets at 160.5-164.2 ppm, and is the most downfield due to strong electron withdrawing *ipso* fluorine atom and the fluorine in the *meta* position. The carbon labeled **c** appearing at 110.2-111.1 ppm is also a doublet of doublets due to the coupling with the two fluorine atoms. Other signals at 110.9, 117.8, 123.4, 129.5, 143.3, 149.7 are identified as singlets and are labeled **g**, **h**, **j**, **i**, **f**, and **k**, respectively.

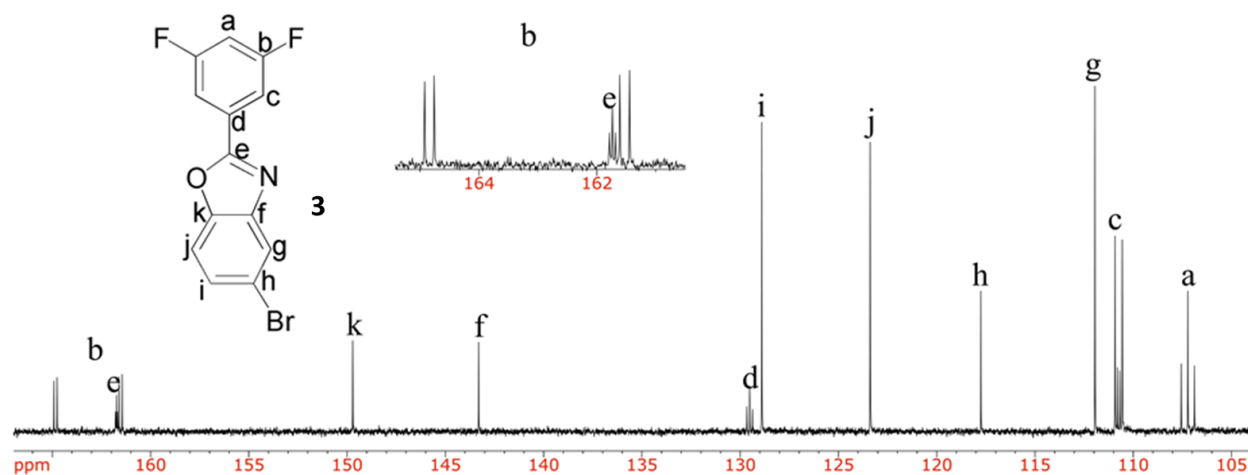
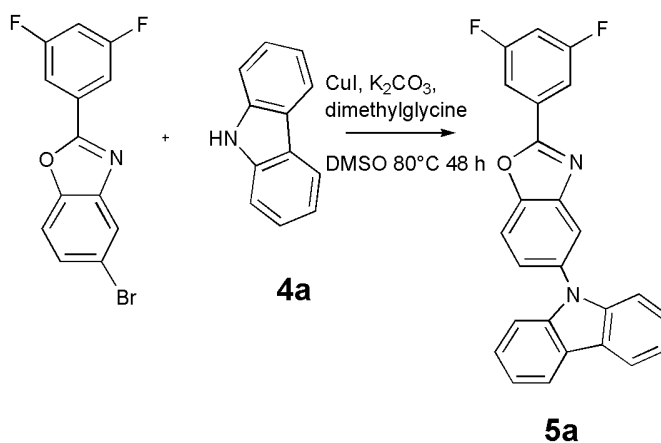


**Figure 8.** 75.5 MHz  $^{13}\text{C}$  NMR ( $\text{CDCl}_3$ ) spectrum of **3**.

### 3.2 Synthesis of BOX-CBZ, 5a

The synthesis of **5a** utilized Ullmann-type, Goldberg coupling reaction of **3** with carbazole, **4a** (Scheme 8).<sup>24, 25</sup> *N,N*-dimethylglycine was used as a ligand, copper (I) iodide a catalyst, and  $K_2CO_3$  as the base. Freshly distilled DMSO solvent was utilized in an effort to prevent poisoning the catalyst. The CuI was activated before use by washing with hot THF in a Soxhlet extractor and used without drying to avoid oxidation. An excess of **4a** (3:1) was used in the reaction to ensure all of **3** was used up in the reaction, and also to reduce the frequency of a competing debromination process. The reaction was complete, as evidenced by GC/MS analysis, after 48 h of reaction, at 80°C. An aliquot from the reaction mixture after 48 h showed less than 1% debromination. Precipitating the reaction mixture in water removed most impurities, except carbazole and some amino acid. The solid obtained after filtration of the precipitate was dissolved in chloroform and mixed with ethanol before slowly removing the chloroform by house vacuum, which allowed the desired product to precipitate while carbazole remained in solution. A second filtration was done to isolate the solids, which were later recrystallized from 50% ethanol-chloroform mixture to give white-pink crystals of **5a** at 87% Yield.



Scheme 8. Synthesis of BOX-CBZ monomer, **5a**

The monomer, **5a**, was analyzed for purity using GC/MS (100 %), melting point 210-212 °C, elemental analysis (Theoretical; C=75.51%, H=3.54%. Found; C=75.48, H=3.58), and NMR spectroscopy. The  $^1\text{H}$  NMR spectrum of **5a** is shown in **Figure 9**.

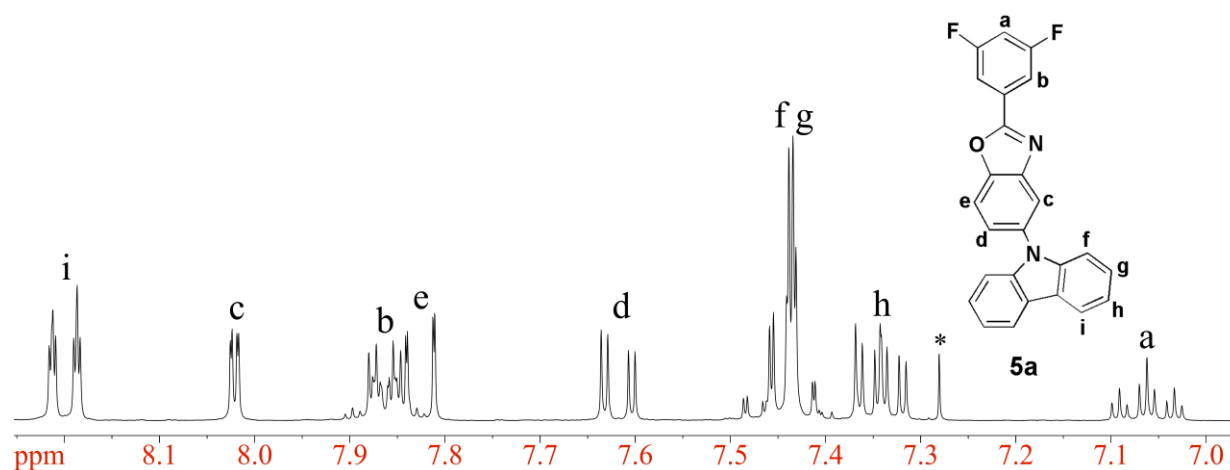


**Figure 9.** 300 MHz  $^1\text{H}$  NMR ( $\text{CDCl}_3$ ) spectrum of **5a**.

As expected, the proton NMR spectrum showed nine unique peaks. The peak at 7.06 ppm is a triplet of triplets and is assigned to proton **a**, between the two fluorine atoms, with coupling constants similar to those observed in **BOX-Br**. Protons **d** and **e** are doublets of doublets and **b** is a multiplet as in **BOX-Br**. New peaks, **e**, **g**, **h** and **i**, from carbazole are introduced into spectrum. The peak labeled **h**, at 7.34 ppm, is a doublet of doublet of doublet due to coupling with two inequivalent protons at ortho positions (**i** and **g**) and with one proton in the meta position, **e**, ( $^3J_{\text{H-H}} = 7.7$ ,  $^3J_{\text{H-H}} = 6.1$ ,  $^4J_{\text{H-H}} = 2.1$ ). The peaks at 7.48-7.40 ppm are multiplets and are assigned to protons **e** and **g**. The peak labeled **d**, at 7.62 ppm is a doublet of doublets due to coupling with **e** and with proton **c**. The peak labeled **e**, at 7.83 ppm is a doublet of doublets. The peak at 7.86 ppm

is assigned to proton **b**, the peak is a multiplet due to coupling with two chemically inequivalent fluorine atoms at the *ortho* and *para* position, and with the proton at *meta* position. At 8.02 ppm is a doublet of doublets which is assigned to proton **c**, the doublet of doublets is due to coupling with protons **d** and with **c**. The signal at 8.20 ppm is assigned to proton **i**, and is a multiplet due to ortho coupling with **h** and also coupling with *meta* and *para* protons (**e**, **g**).

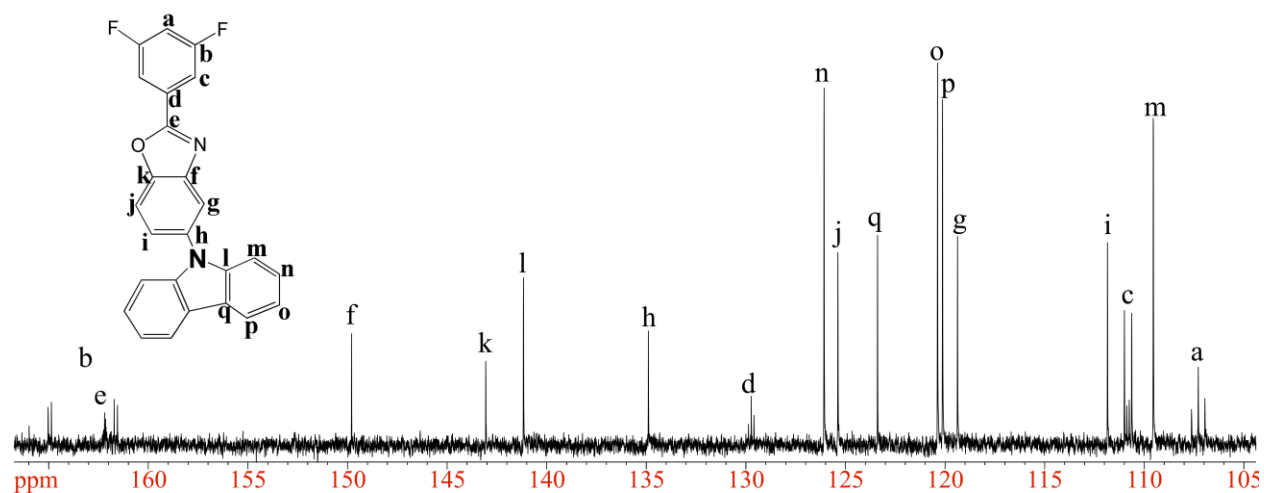


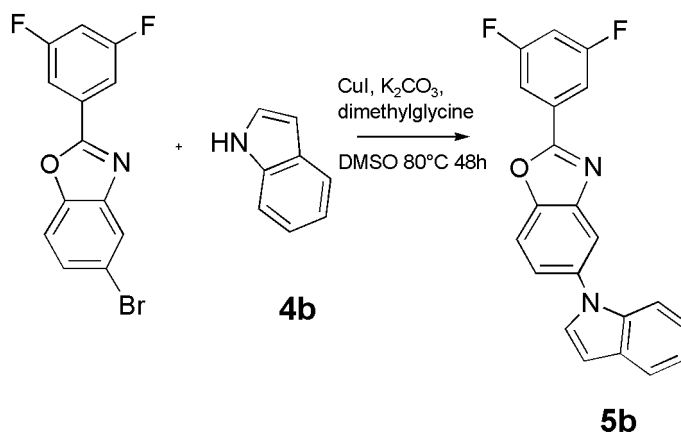
**Figure 10.** 75.5 MHz  $^{13}\text{C}$  NMR ( $\text{CDCl}_3$ ) spectrum of **5a**.

As expected, the  $^{13}\text{C}$  NMR spectrum (**Figure 10**) showed seventeen chemically inequivalent carbons. The new carbons introduced to the structure are labeled **l**, **m**, **n**, **o**, **p** and **q**. The carbon signals, **a**, **d**, and **e**, appearing at 107.3 ppm, 129.7 ppm and 162.2 ppm, respectively, are triplets due to coupling with the two fluorine atoms as in **BOX-Br**. The signals from the carbon atoms labeled **b** and **c** are doublets of doublets at 160.4-164.1 ppm and 110.1-111.3 ppm respectively. All other carbon signals appear as singlets at 109.6, 110.8, 111.9, 119.4, 120.1, 120.4,

123.4, 125.4, 126.1, 134.9, 141.2, 143.01, 149.8, 151.5, and 163.3 ppm and are assigned as shown in **Figure 10**.

### 3.3 Synthesis of BOX-IND, **5b**

**BOX-IND, 5b**, was synthesized by the coupling reaction of **3** with excess indole, **4b**, in the presence of CuI catalyst, *N,N*-dimethylglycine ligand, and potassium carbonate (Scheme 9).<sup>24</sup>  
<sup>25</sup> The reaction was complete in 24 h with less than 1% of **3** debrominated. The reaction mixture was precipitated and salted out due to the high solubility of **5b** in DMSO. Excess indole was removed by triturating the mixture in warm water, which melted and washed out any remaining indole. The product was then recrystallized two times from 50% ethanol-chloroform to obtain brownish crystals of **5b** in 85 % yield.



**Scheme 9.** Synthesis of **BOX-IND, 5b**.

The product was characterized by melting point (130-132°C), GC/MS (100 %), elemental analysis, and NMR spectroscopy. The <sup>1</sup>H NMR spectrum is shown in **Figure 11**.

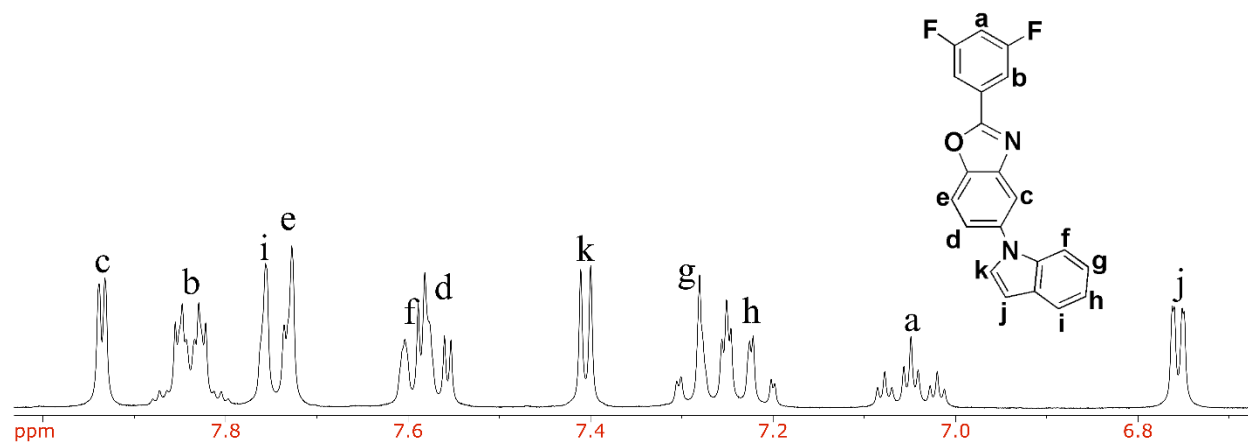


**Figure 11.** 300 MHz  $^1\text{H}$  NMR ( $\text{CDCl}_3$ ) spectrum of **BOX-IND** monomer, **5b**.

The signal from proton marked **j**, at 6.76 ppm is a doublet of doublets due to coupling with **k** and **j** ( $^4J_{\text{H-H}} = 3.2$ ,  $^5J_{\text{H-H}} 0.6$ ). The peak at 7.22 is assigned to proton labeled **h**, this is a multiplet due to coupling with protons **i**, **g**, and **f**. Signal from proton **g** appears as a multiplet due to coupling with proton **f**, **h** and **i**. The proton **j**, at 7.41 is a doublet of doublets due to coupling with **k** ( $^3J_{\text{H-H}} = 3.3$  Hz) and with **i**. Other peaks and their coupling are identical to those observed in **BOX-Br** and **BOX-CBZ**.

The  $^{13}\text{C}$  NMR spectrum of **BOX-IND** is shown in **Figure 12**. Eight new carbon atoms from indole are introduced into the **BOX-Br** structure. Their signals are assigned as **r**, **m**, **s**, **p**, **o**, **q**, **n** and **r**, appearing at 103.9, 110.3, 116.4, 121.2, 122.0, 123.1, 129.4, 137.2 ppm, respectively.

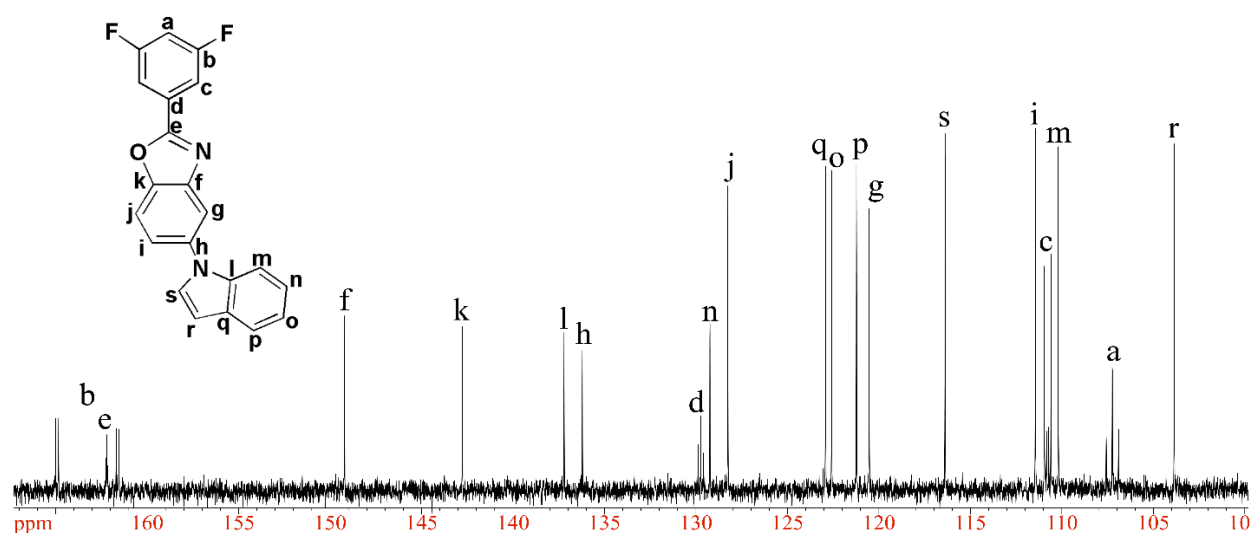
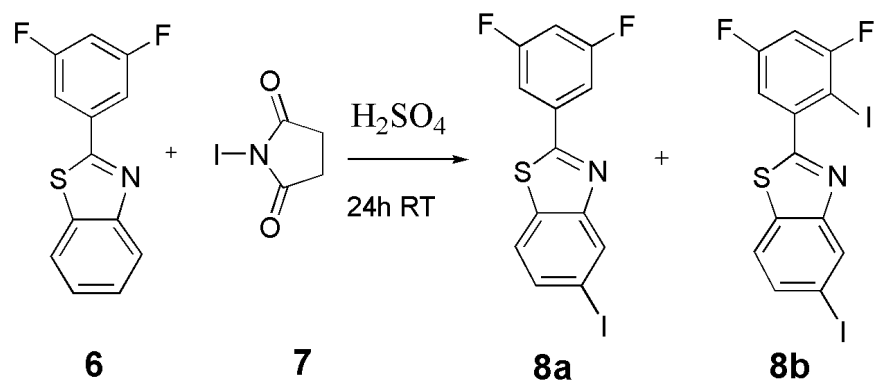


**Figure 12.** 75.5 MHz  $^{13}\text{C}$  NMR ( $\text{CDCl}_3$ ) spectrum of **BOX-IND monomer**.

### 3.4 Iodination of 2-(3,5-Difluorophenyl)-benzothiazole, **BTZ** (**6**)

2-(3,5-Difluorophenyl)-benzothiazole, **6**, was synthesized via a previously reported route involving the reaction of 3,5-difluorobenzoic acid with 2-aminothiophenol in the presence of polyphosphoric acid. The proton and carbon NMR data agreed with the literature values. Iodination was performed with *N*-iodosuccinimide, **7**, (**NIS**) in concentrated sulfuric acid (**Scheme 10**). **NIS** and **BTZ** were first dissolved separately in sulfuric acid and mixed with vigorous stirring to reduce local concentration effects that might cause multiple iodinations to occur. The reaction was allowed to stir at room temperature for 24 h, at which point GC/MS analysis of an aliquot showed 78% mono (**8a**) and 11% diiodinated (**8b**), species present. The reaction mixture was precipitated from excess water and washed with sodium bicarbonate solution to remove the acid. The product was recrystallized from a mixture of ethanol, toluene, and chloroform (1:1:8) to afford 52% yield of **8a**.



**Scheme 10.** Synthesis of **BTZ-I, 8a**.

The proton NMR spectrum of **8a** displayed four peaks as shown in **Figure 13**. The peak labeled **a**, at 6.97 ppm, is a triplet of triplets, and is assigned to the proton on the upper phenyl ring between the two fluorine atoms. The triplet of triplets is due to the coupling with the two fluorines with two chemically equivalent fluorine atoms ( $^3J_{H-F} = 8.5$  Hz) and the two protons at the *meta* position, with equal coupling constants ( $^4J_{H-H} = 2.4$  Hz). The signal from proton **b** appears as a multiplets while proton **c** showed a singlet. Protons labelled **e** and **d** showed overlapping resonances, however their integration showed two protons. All the protons are assigned as shown in **Figure 13**.

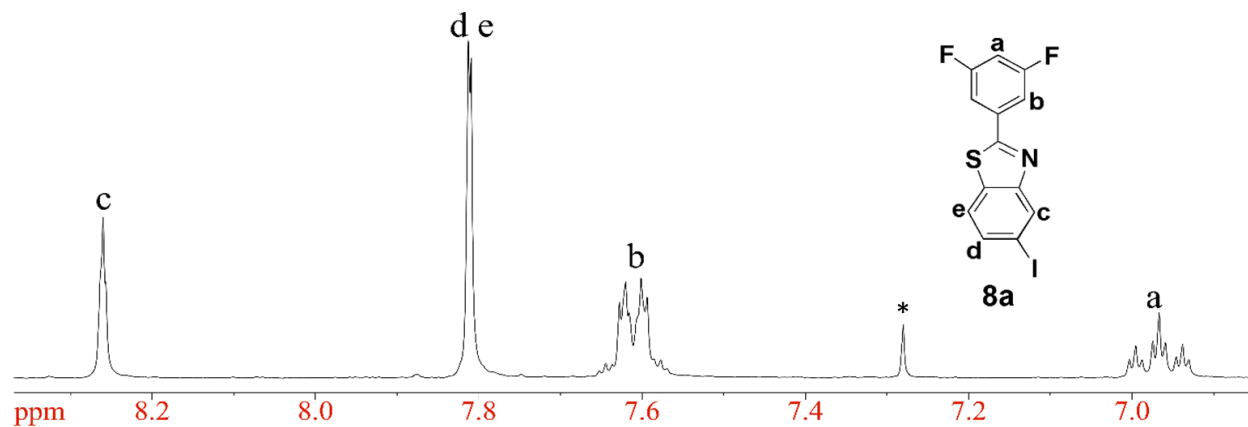
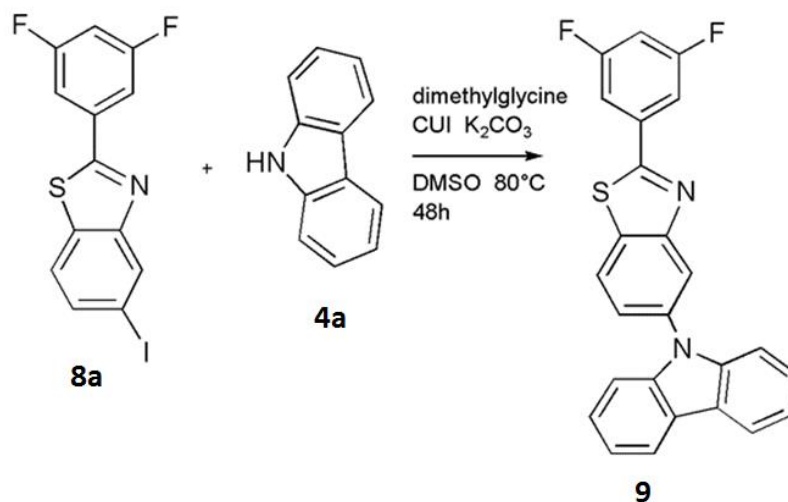


**Figure 13.** 300 MHz  $^1\text{H}$  NMR ( $\text{CDCl}_3$ ) spectrum of **BTZ-I, 8a**

### 3.5. Synthesis of **BTZ-CBZ, 9**

Monomer **9** was synthesized via a coupling reaction of **BTZ-I, 8a**, with **4a** (Scheme 11). The reaction was facilitated by a CuI catalyst and *N,N*-dimethylglycine ligand while  $\text{K}_2\text{CO}_3$  was used as the base. The reaction was carried out in DMSO solvent.<sup>24, 25</sup> Excess carbazole was used to reduce de-iodination of **BTZ-I**. The reaction was complete in 24 h with less than 0.5% de-iodination. The reaction mixture was precipitated from DI water to remove excess  $\text{K}_2\text{CO}_3$  and CuI. The mixture was filtered and the resulting solid was dissolved in chloroform and filtered again to remove any remaining amino acid. Ethanol was added to the mixture and the chloroform was removed under reduced pressure to allow the insoluble **BTZ-CBZ** to crystallize. The monomer was further purified by recrystallization from 20% ethanol in chloroform to afford 78% yield of **BTZ-CBZ**.



**Scheme 11.** Synthesis of **BTZ-CBZ** monomer, **9**.

The purity of the product was analyzed by GC/MS (100%), NMR spectroscopy and elemental analysis. The  $^1H$ -NMR spectrum of **9** is shown in **Figure 14**.

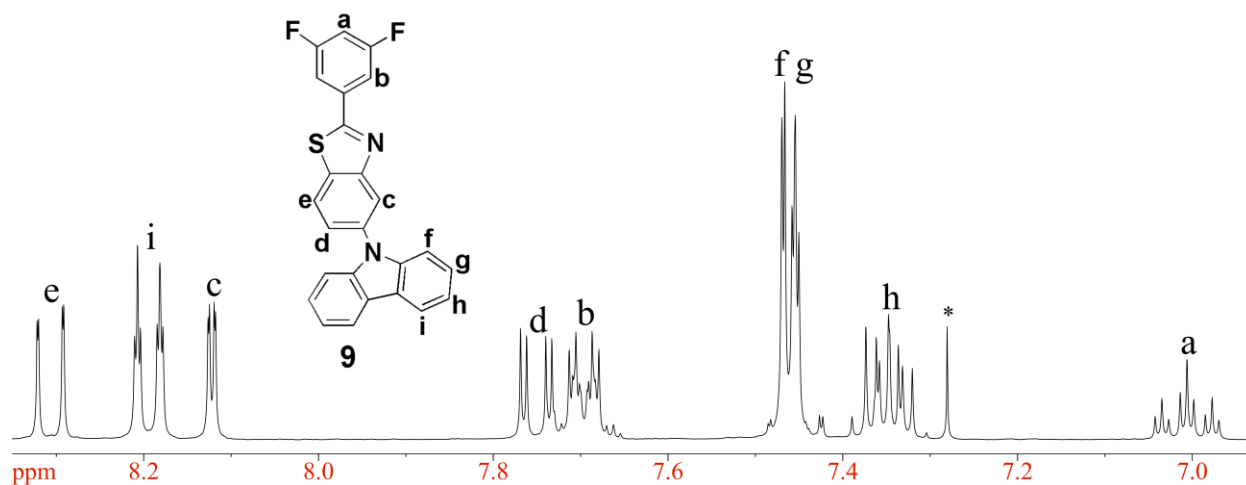


**Figure 14.** 300 MHz  $^1H$  NMR ( $CDCl_3$ ) spectrum of **9**

New peaks arising from the introduction of carbazole into **BTZ-I** are labelled **f**, **g**, **h**, and **i**. The signal for the proton labeled **h** appears at 7.35 ppm and is a doublet of doublet of doublets due to coupling with two inequivalent *ortho* protons, **i** and **g** and with the *meta* proton, **f**. The signals for the protons labelled **f** and **g**, appearing at 7.41-7.44, are multiplets due to coupling with each other and with protons **h** and **i**. Proton **i** is also a multiplet at 8.19 ppm.

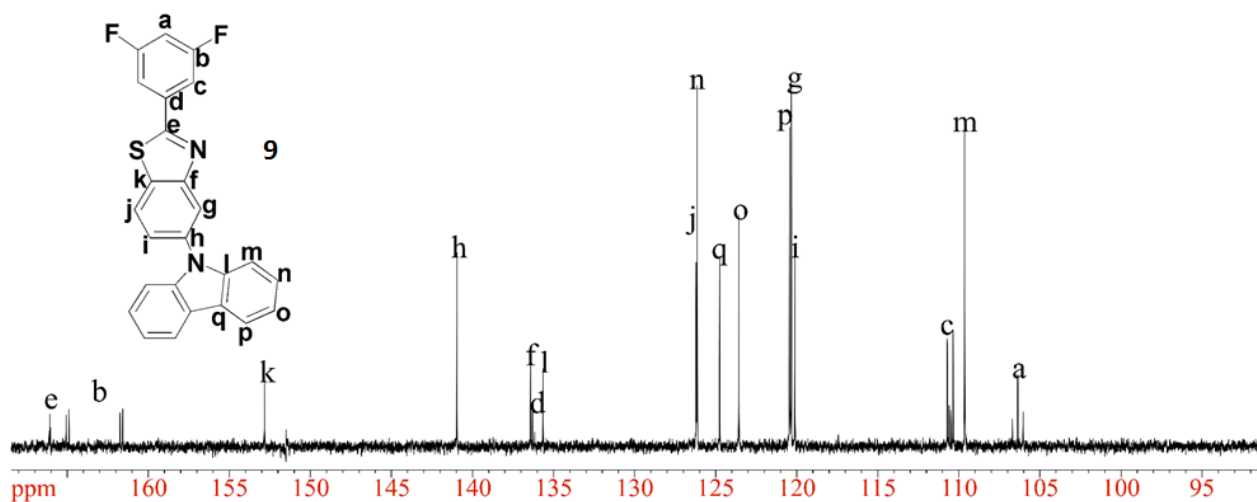


**Figure 15.** 75.5 MHz <sup>13</sup>C NMR (CDCl<sub>3</sub>) spectrum of **9**

The <sup>13</sup>C NMR spectrum (**Figure 15**) clearly shows the carbazole peaks **l**, **m**, **n**, **o**, **p**, and **q** that were introduced into the **BTZ-I** structure and no C-I signal, ~ 95 ppm.

### 3.6 UV and Fluorescence of BTZ-CBZ, BOX-CBZ and BOX-IND monomers

UV and Fluorescence data of the three monomers were acquired in THF at a concentration of 20  $\mu\text{M}$ . The data are presented in **Figures 16a** and **16b**, respectively. **BTZ-CBZ** showed the strongest absorption with  $\lambda_{\text{max}}$  at 341 nm. The **BOX-CBZ** absorption intensity was a little less than that of **BTZ-CBZ** with a maximum absorption at 339 nm while the **BOX-IND** monomer showed the least intense absorption with a  $\lambda_{\text{max}}$  at  $\sim$  339 nm.

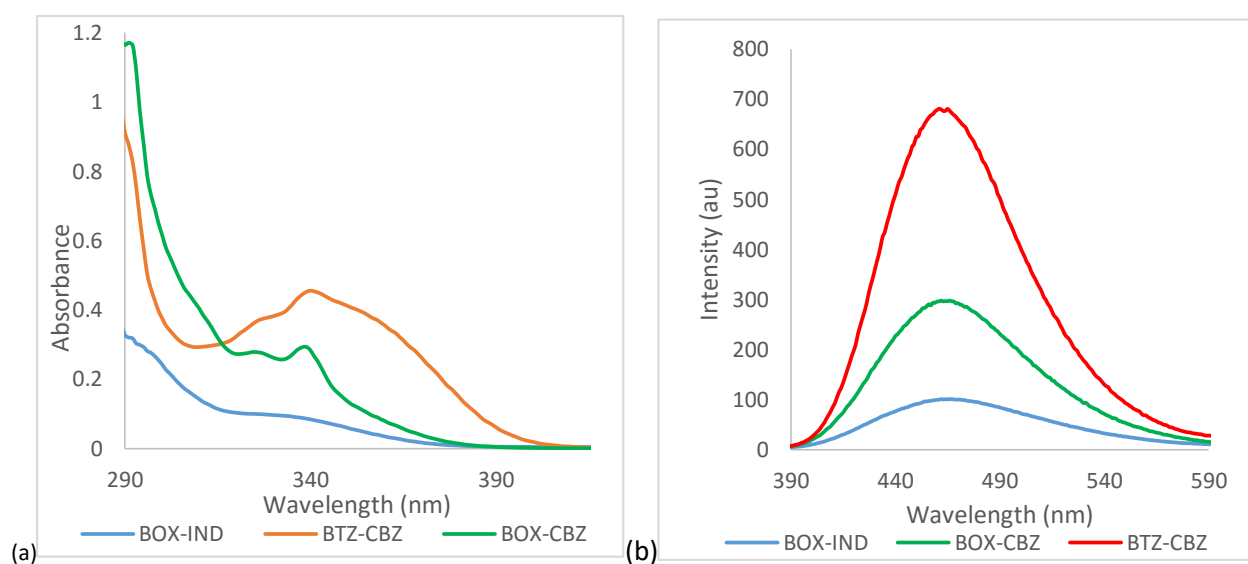


**Figure 16.** (a) Absorption and (b) Fluorescence spectra of **BTZ-CBZ**, **BOX-CBZ** and **BOX-IND** in THF, excited at 310nm.

All three monomers showed broad, but strong emission centered at about 460 nm. **BTZ-CBZ** monomer showed the highest in emission intensity while **BOX-IND** had the lowest intensity which may be due to weaker electron donating group, indole. Varying the excitation wavelength from 250 nm to 340 nm changed the intensity of fluorescence, but the maximum emission

wavelength remained unchanged. For all three monomers the highest fluorescence intensity was observed between excitation wavelengths of 300-320 nm.

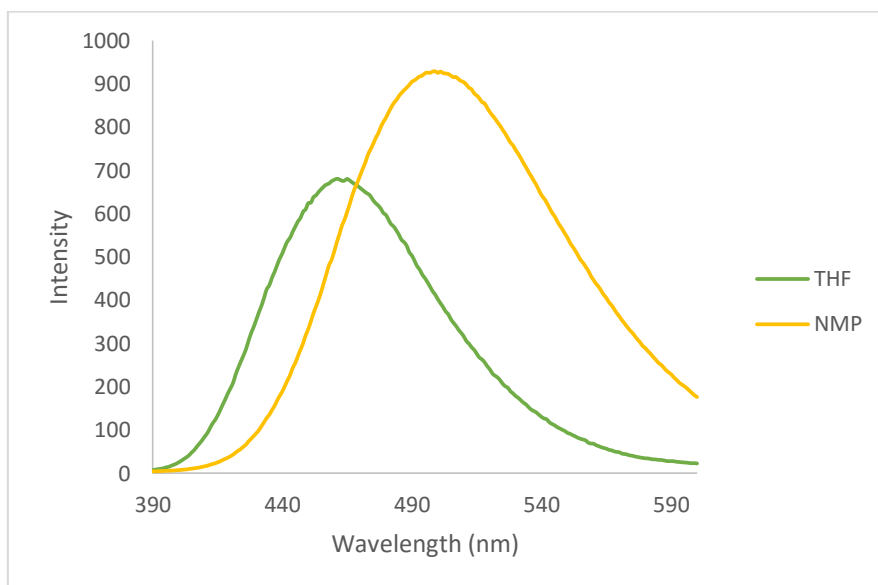
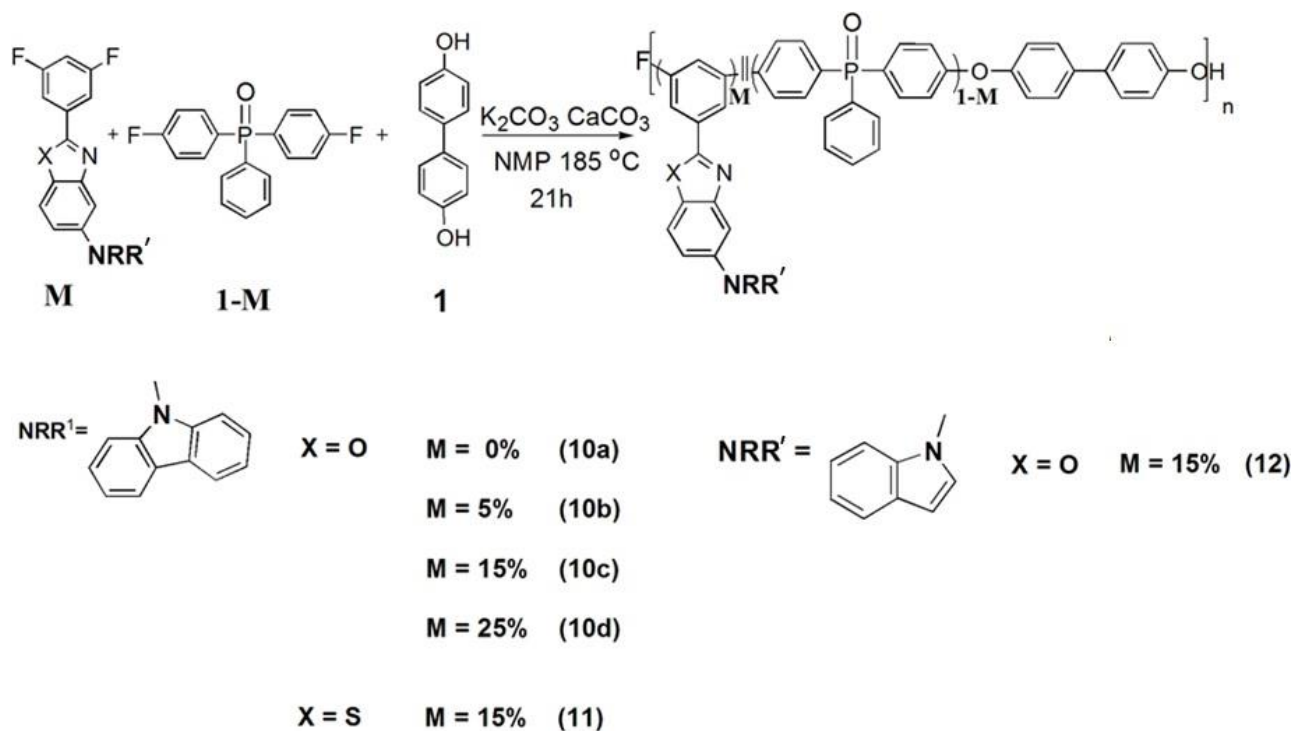


**Figure 17.** Fluorescence spectra of **BTZ-CBZ, 9**, in THF and in NMP, excited at 300 nm.

When the fluorescence of **BTZ-CBZ** monomer was compared in NMP and in THF solvents (**Figure 17**), the more polar solvent, NMP, caused a large shift in emission wavelengths towards longer wavelengths. This is bathochromic shift, which is observed in  $\pi$ - $\pi^*$  transitions, and is caused by attractive polarisation forces between the solvent and the chromophores which lower the energy levels of both the excited and unexcited states causing the shift to lower energy, red shift in fluorescence.

### 3.7. Synthesis of copolymers 10a-10d, 11, and 12

Polymers **10a-10d**, **11**, and **12** were synthesized via typical Nucleophilic Aromatic Substitution (NAS) polycondensation reactions (**Scheme 12**).<sup>16, 17</sup>  $K_2CO_3$  and  $CaCO_3$  were used to deprotonate 4,4'-biphenol with  $CaCO_3$  also helping to remove active fluoride by-products from the reaction mixture. A polar aprotic solvent, NMP, was used to facilitate the reaction.



**Scheme 12.** Synthesis of polymers **10a-10d**, **11**, and **12**.

The synthesis of homopolymer **10a** was achieved by the reaction of bis-(4-fluorophenyl)phosphine oxide and 4,4'-biphenol in the presence of  $K_2CO_3$  and NMP. The reaction mixture precipitated well from DI water to give a white precipitate. The polymer formed clear and flexible films when cast from NMP solutions of the polymer on a glass slide. **Figure 18** displays

the  $^{13}\text{C}$  NMR spectrum of **10a** (top), which clearly shows 12 signals after completion of the reaction. The signals for carbons labeled **r**, **s**, **t**, **u**, **v**, **w**, **x** and **y**, are assigned to the phosphine oxide unit in the polymer, and are doublets due to coupling with phosphorus.

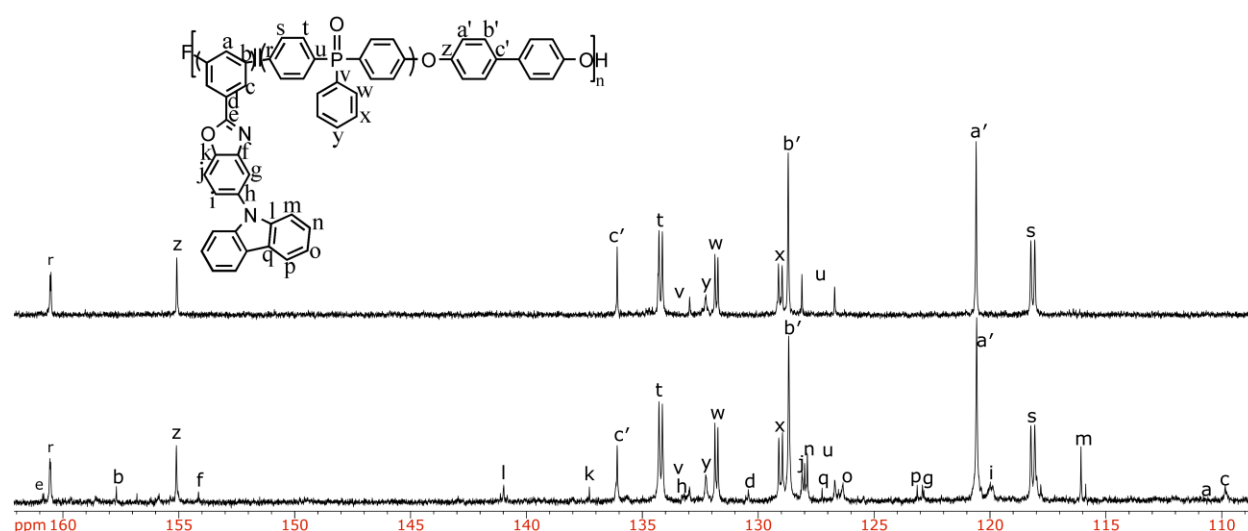


**Figure 18.**  $^{13}\text{C}$  NMR (NMP/DMSO- $d_6$ ) spectral overlay of **10c** (bottom) and **10a** (top).

Polymers **10b**, **10c**, and **10d** were synthesized by copolymerization of 5%, 10% and 15% of monomer **5a**, respectively, with *bis*-(4-fluorophenyl)phenylphosphine oxide and 4,4'-biphenol as the nucleophilic reaction partner. The reactions were carried out with  $\text{K}_2\text{CO}_3$  and  $\text{CaCO}_3$  as base, and NMP solvent, at 185 °C for 21 h. The three polymers were isolated as white solids upon precipitation from DI water. Further purification was achieved by reprecipitation after dissolving the polymers in NMP, and adding the solution, drop-wise, into vigorously stirred DI water. The molecular weights of the three copolymers could not be determined due to their lack of solubility in the currently utilized SEC solvent, THF/5% acetic acid. Polymers **10a-10d** showed good

solubility in NMP and dimethylacetamide (DMAC) solvents, but were insoluble in DMSO, chloroform, and THF.

The reaction progress and polymer structure was confirmed by  $^{13}\text{C}$  NMR spectroscopy, which showed clear changes in the signals originating from the carbon between the two fluorine atoms, a triplet at 105 ppm, labelled **a** in the monomer. The signal changed from a triplet to a doublet with displacement of one fluorine atom, then to a singlet when both fluorine atoms were displaced, and the reaction was complete. Other peaks showed subtle changes in the spectrum compared to their corresponding initial units due to formation of ether bonds in the polymerization process. The  $^{13}\text{C}$  NMR spectrum (**Figure 18**) showed four tall peaks labelled **z**, **a'**, **b'**, and **c'** from the biphenol ring where **a'** and **b'** are the tallest and represent the signals from the two sets of equivalent carbons. The signals from the phosphine oxide unit, **r**, **s**, **t**, **u**, **v**, **w**, **x** and **y** appear as doublets due to coupling with phosphorus, while those from the chromophore unit, **5a** are singlets and weak due to their low percentage in the polymer. The peaks for the respective carbon atoms are assigned as shown in **Figure 18**.

Polymer films were prepared by dissolving the copolymers in NMP and then casting onto glass slides. The copolymers **10b** and **10c**, containing 5% and 15% **BOX-CBZ** gave flexible and transparent films, while films from **10d**, having 25% of **5a**, were brittle.

Synthesis of copolymer **11** was done in the same way as all the other polymers, but with 15% of monomer **9**. To ensure purity, polymer **11** was dissolved in NMP solvent and left to settle overnight before glasswool filtration and reprecipitation. The polymer showed good solubility in NMP, but was insoluble in chloroform, DMSO, and THF solvents. A polymer film was cast from NMP solvent on a glass film, which showed a strong attraction to the glass slide. However, soaking

the glass slide in water allowed the film to be removed. The UV and fluorescence data were acquired in NMP solvent and from the polymer film.

The polymer structure was also confirmed by NMR analysis (**Figure 19**) in a NMP and DMSO- $d_6$  solvent mixture (2:5). Also,  $^{13}\text{C}$  NMR spectroscopy was used to monitor the progress of the polymerization reactions. A triplet signal, usually appearing at about 105 ppm in monomer **9**, changes to a doublet with displacement of one fluorine atom, and finally, to a singlet when the reaction is complete. Also, the polymer showed slight changes in the chemical shifts compared to their initial units due to the formation of ether bonds.

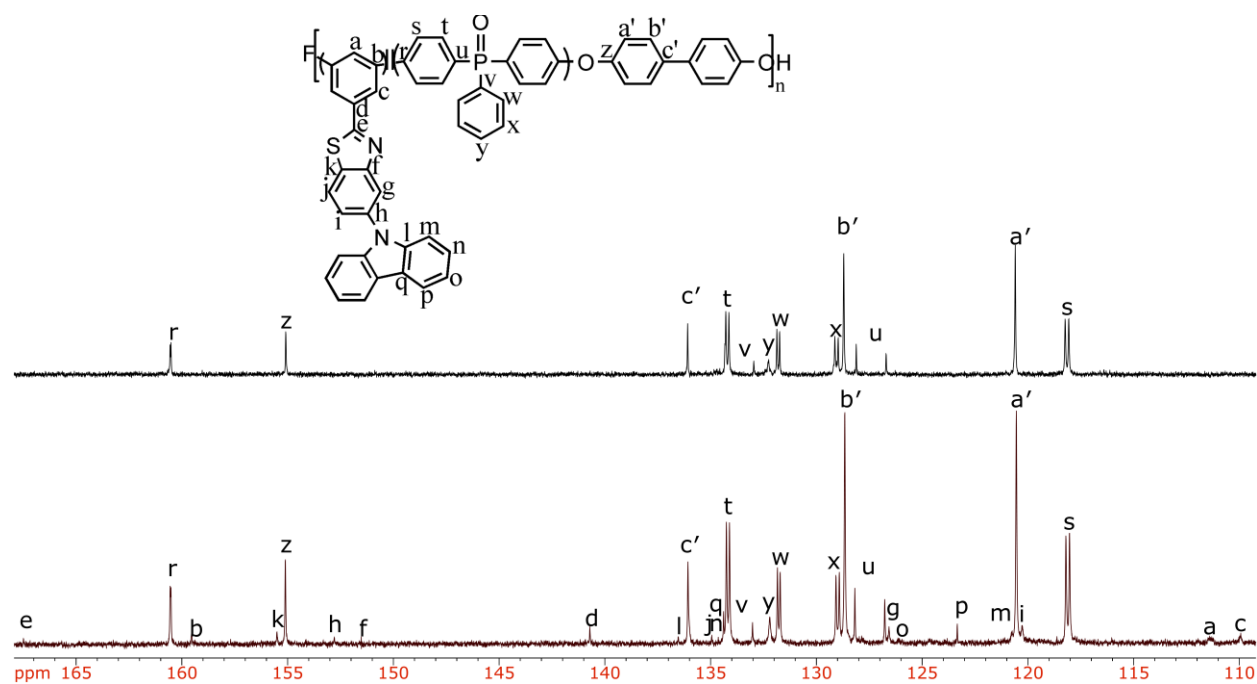


**Figure 19.**  $^{13}\text{C}$  NMR (NMP/DMSO- $d_6$ ) overlay of **11** and **10a**.



### 3.11 Thermal Analysis

The polymer thermal properties were evaluated using Differential Scanning Calorimetry (DSC) and Thermogravimetric Analysis (TGA). The TGA thermograms of all the polymers under a nitrogen atmosphere are shown in **Figure 21**, and the data are summarized in **Table 1**. All polymers showed a single-step degradation with high thermal stabilities under nitrogen. Copolymers **10b-10c** showed a decrease in degradation temperature, evidenced by lower 5% degradation temperatures,  $T_{d-5\%}$ , with an increased percentage of **BOX-CBZ** monomer. This is attributed to the lower thermal stability of **BOX-CBZ** monomer, which decreases the overall polymer stability when more is incorporated. The homopolymer **10a** was the most stable with  $T_{d-5\%}$  in excess of 590 °C

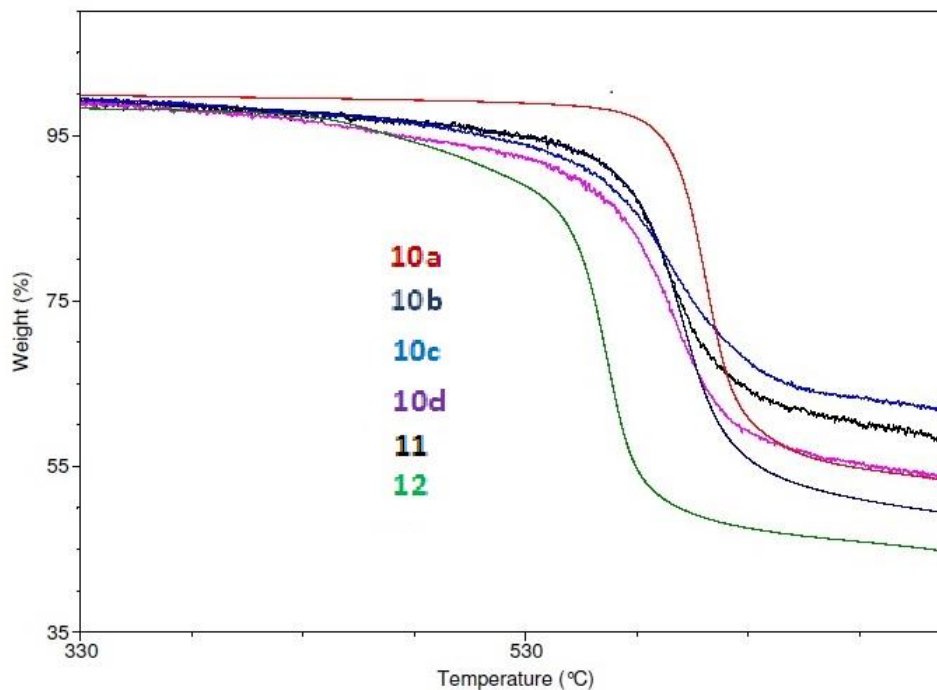


**Figure 21.** Overlay of TGA traces of the polymers **10a-10d**, **11**, and **12**.

Polymer	T <sub>g</sub> °C	T <sub>d-5%</sub> °C
Homopolymer (10a)	232	590
5% BOX-CBZ (10b)	232	517
15% BOX-CBZ (10c)	236	507
25% BOX-CBZ (10d)	235	472
15% BTZ-CBZ (11)	243	525
15% BOX-IND (12)	210	467

**Table 1.** Glass transition temperatures, T<sub>g</sub>, and 5% degradation temperatures, T<sub>d-5%</sub>, under nitrogen atmospheres for polymers **10a-10d**, **11**, and **12**

An overlay of the DSC traces of the six polymers is shown in **Figure 22** and summarized in **Table 1**. The DSC traces clearly indicate that polymer **12** has the lowest glass transition temperature of all the polymers; this is attributed to the asymmetrical monomer structure. **BTZ-CBZ** copolymer showed the highest glass transition temperature, 243 °C this is due to the highly rigid polymer structure, which limits rotation around sigma bonds in the polymer backbone. Polymers **10b-10d** showed increasing glass transition temperatures from 5% to 25% monomer concentration. This is due to an increase in the more bulky pendent group which makes the polymer more rigid and hence raising the glass transition temperature. DSC showed no other polymer thermal transitions and hence the polymer were completely amorphous. The homopolymer, **10a** also had a high glass transition temperature of 232 °C, which may be due to decreased free volume which raises the glass transition temperature.

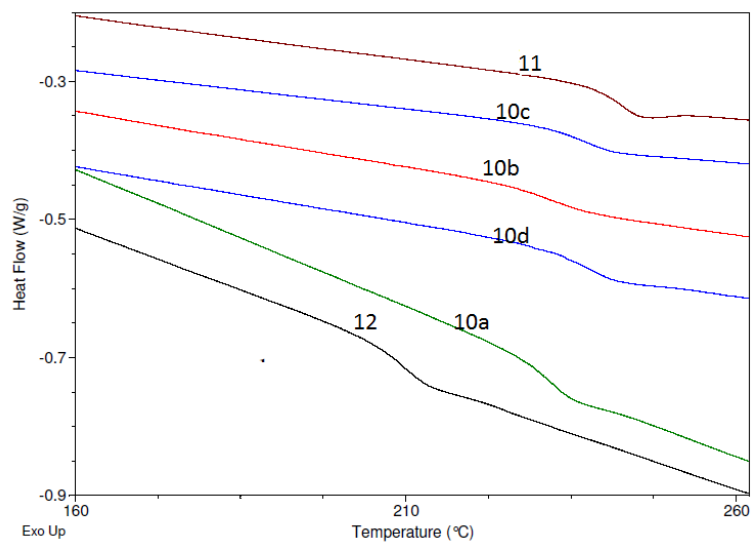


**Figure 22.** DSC traces of polymers **10a-10d**, **11** and **12** under nitrogen at a heating rate of 10 °C/min.

#### 4. Absorption and Emission

Polymer absorption and fluorescence data were acquired in NMP solutions at a concentration of 20 micromolar as well as from the polymers in film form. **Figure 23** illustrates the UV and fluorescence spectra of polymers **10b-10d** acquired in NMP solutions. The copolymers showed strong absorptions from 262 nm to 344 nm. At 300 nm to 345 nm, the decrease in intensities of absorption follows the order of the decrease in percentage of chromophore in the polymer, this indicates that the absorption above 300 nm is attributed to monomer present in the polymer.

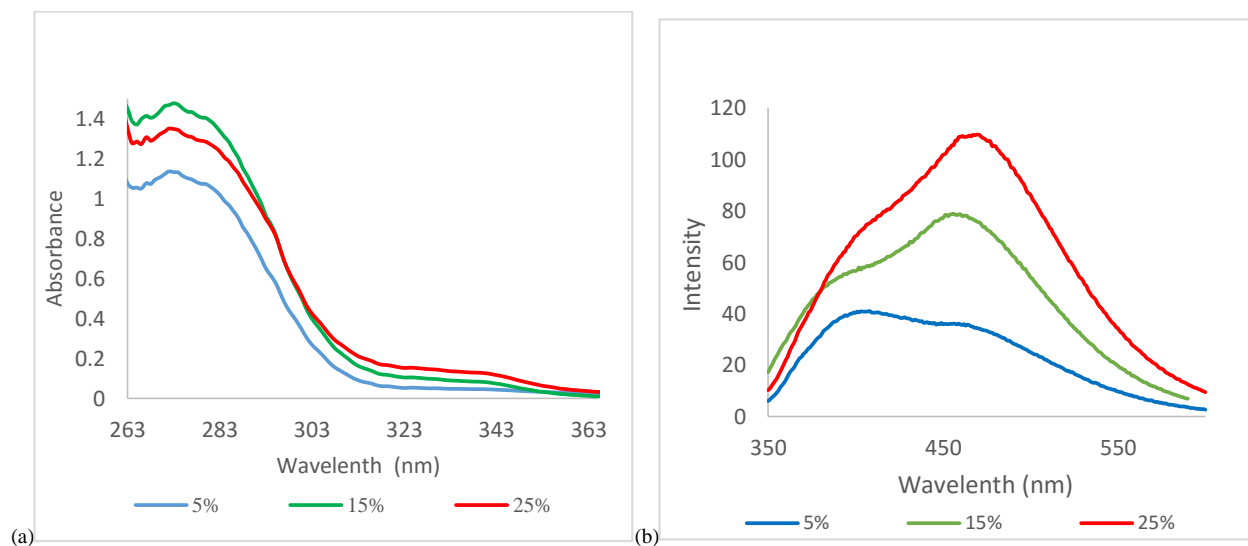


**Figure 23.** Absorption (a) and emission (b) spectra of the **BOX-CBZ** copolymers, **10b** (5 %), **10c** (15 %), and **10d** (25 %), excited at 315 nm.

An overlay of fluorescence spectra of **10b-10d** is shown in **Figure 23b**. The 15% and 25% copolymers showed maximum fluorescence peaks at 473 nm. Polymer **10d**, containing 25 % chromophore showed the highest fluorescence intensity due to high percentage of chromophore in

the polymer. The 5% copolymer, **10b** showed the weakest fluorescence also due to low percentage of the chromophore. Interestingly, the emission maximum for **10b** was centered at ~ 400 nm, with a broad secondary peak centered at ~ 460 nm.

The solution fluorescence data of homopolymer, **10a** and copolymers containing 15% chromophore, **10c**, **11**, and **12** in NMP is shown in **Figure 24a**. The **BTZ-CBZ** copolymer, **11**, showed nearly four and a half times higher emission intensity than the **BOX-CBZ** copolymer, while the **BOX-IND** copolymer, **12** had the weakest fluorescence. Polymer **11** had a maximum intensity at 491 nm with no shoulder peaks. Polymer **10c** had a maximum fluorescence at 473 nm and a smaller peak at 403 nm. Polymer **12** showed the weakest fluorescence and lowest emission maximum, ~ 416 nm.

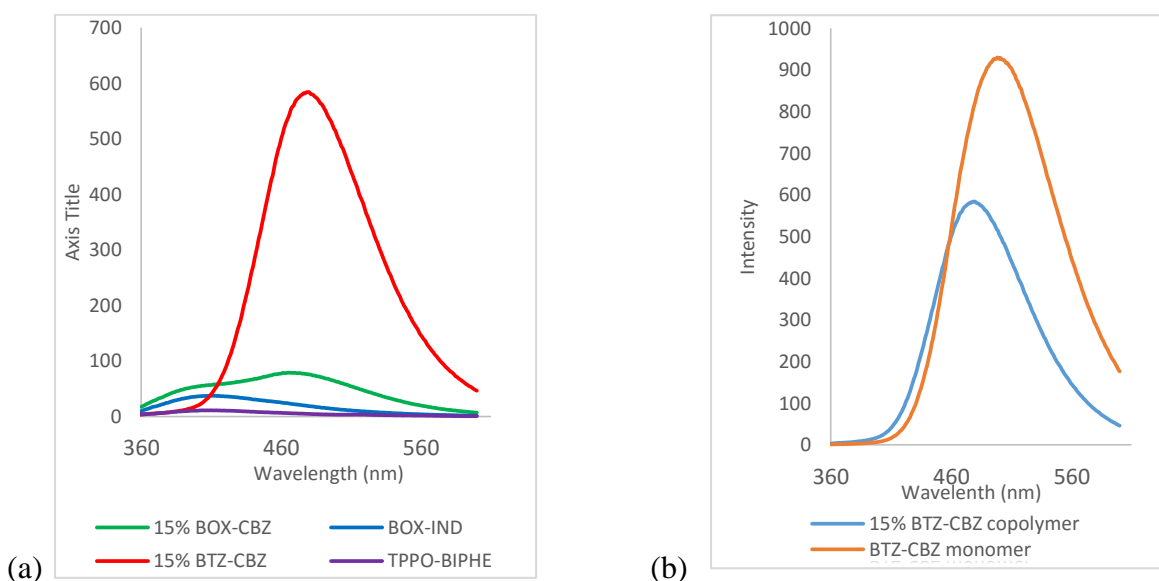


**Figure 24.** (a) Fluorescence of copolymers containing 15% **BOX-CBZ**, **BOX-IND**, **BTZ-CBZ**, and **TPPO-BIPHE** homopolymer in NMP. (b) Fluorescence of monomer **9** and polymer **11** excited at 315 nm in NMP solution.

All of the polymers showed significant differences in fluorescence when compared to their corresponding monomers in NMP. Monomer **9**, **Figure 24b**, showed maximum fluorescence wavelength centered at 500 nm, while its copolymer, **11**, showed maximum wavelength at 481 nm in NMP solvent.

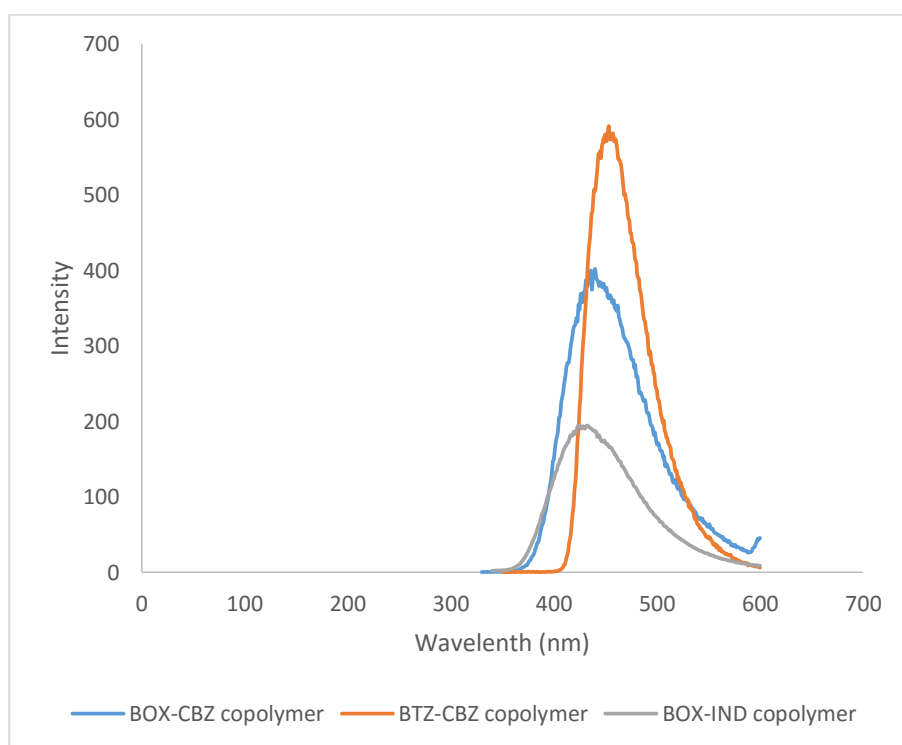


**Figure 25.** Fluorescence from films of polymers **10c**, **11**, and **12**, containing 15% chromophore, excited at 315 nm

Fluorescence of the three copolymers was also measured on films cast onto glass slides. The films were excited at different wavelengths (280-350 nm). In all polymers, the highest intensities were observed with an excitation wavelength of 315 nm. The fluorescence of polymer films from excitation wavelength of 315 nm is shown in **Figure 25**. The **BTZ-CBZ** copolymer showed a narrow and high intensity fluorescence at about 451 nm. The **BOX-CBZ** copolymer

showed a weaker and broader emission at 432 nm, while the **BOX-IND** copolymer had the weakest emission, which was centered at 430 nm.

Comparing the fluorescence of polymer in films to their solutions in NMP, a large shift to longer wavelengths is observed in solvent which is due to attractive polarization forces between the solvents and the chromophores, which lower the energy levels excited states causing a 'red shift'.

**Figure 26** shows the photoluminescence of polymer **11** cast on a glass slide under excitation from a UV lamp at a wavelength of 361 nm. The polymer shows a strong and blue fluorescence which indicate a potential for OLED application.



**Figure 26.** Photo of polymer **11** emitting in the blue region of the spectrum, excited by UV lamp at 361 nm.

#### 4. CONCLUSION

Fluorescent monomers 9-[2-(3,5-Difluorophenyl)-benzoxazol-5-yl]-9H-carbazole (**BOX-CBZ**), 9-[2-(3,5-Difluorophenyl)-benzothiazol-5-yl]-9H-carbazole (**BTZ-CBZ**), and 2-(3,5-Difluorophenyl)-5-indol-1-yl-benzooxazole (**BOX-IND**), were successfully synthesized via copper (I) catalyzed amination reactions of either 5-Bromo-2-(3,5-difluorophenyl)-benzooxazole and 5-Bromo-2-(3,5-difluorophenyl)-benzothiazole. All the monomers showed strong absorption at wavelengths of 280 nm to 340 nm. The fluorescence analysis showed strong emission at about 463 nm in THF and 470 nm to 502 nm in NMP. Fluorescence of the three monomers in THF solution showed different emission intensities, but very similar emission wavelengths. The monomer solutions in NMP solvent showed significant differences; **BTZ-CBZ** emitted with a strong intensity at 501 nm, **BOX-CBZ** at 505 nm and **BOX-IND** at 509 nm.

The monomers were successfully copolymerized with *bis*-(4-fluorophenyl)-phenyl phosphine oxide and 4,4'-Biphenol via typical NAS reactions. The copolymers showed good solubility in NMP and dimethylacetamide (DMAC) solvents at room temperature, but were insoluble in most other solvents such as DMSO, THF, and toluene. All polymers, with the exception of the 25% **BOX-CBZ** copolymer, formed good films when cast on glass slides.

The polymers showed high heat stability with 5 % weight loss temperatures in excess of 450°C and glass transition temperatures above 200 °C. The **BTZ-CBZ** copolymer showed both the highest glass transition (number here) and degradation temperature (number here) while the **BOX-IND** copolymer showed the lowest  $T_g$  (insert number here). The **BOX-CBZ** copolymers showed an increase in  $T_g$  with an increase in the percentage of the **BOX-CBZ** monomer incorporated into the polymer. Most likely this is due to the bulky pendent group in the monomer which hinders the rotation around sigma bonds. The same polymers show decreasing thermal

stability with an increase in the percentage of **BOX-CBZ** monomer, thus, it can be inferred that the **BOX-CBZ** monomer is susceptible to heat and therefore lowers the polymer stability at high temperatures.

All of the polymers showed strong absorptions between 290 nm and 340 nm when measured in NMP solution. Fluorescence spectra showed distinct emission peaks at 481nm for **11**, 473 nm for **10c** and 410 nm for **12**. Analysis of the fluorescence data from polymer films showed true blue emission from the **BTZ-CBZ** copolymer, with a maximum wavelength of 451 nm. The **BOX-CBZ** and **BOX-IND** copolymers emitted at 432 nm and 430 nm, respectively.

## 5. PROPOSED WORK

Current studies have shown the potential for development of blue OLED emitters based on benzoxazole and benzothiazole. The monomers can be easily polymerized to form PAE-based fluorescent polymers for OLED applications.

In order to improve the monomer synthesis and percent yields, other methods of halogenation need to be explored to avoid the formation of dihalogenated products. The amination reaction also needs to be optimized by using other catalysts or different routes of synthesis. Other synthetic routes also need to be investigated to be able to attach other heterocyclic species to the monomer. Polymerization reactions also need to be investigated to determine better ways of eliminating fluoride ions formed during the reaction which may be causing degradation of monomers.

To obtain different colors from the polymer fluorescence, other electron rich groups and amines need to be investigated to determine their donor-acceptor properties and emission wavelengths when attached to acceptor-type monomers.

The current study makes use of benzoxazole and benzothiazole pendent to the polymer chain, as such, the “inline” versions of **BTZ** and **BOX** are also potential candidates for fluorescent materials and need to be studied to determine their potential for OLED applications.

## 6. REFERENCES

1. Li, Z. R.; Meng, H. *Organic Light-Emitting Materials and Devices*; CRC/Taylor & Francis: Boca Raton, FL, **2007**; pp. 2–17.
2. Kafafi, Z. *Organic electroluminescence*; CRC Press/Taylor & Francis: Boca Raton, FL, **2005**; pp. 1-8.
3. Templier, F. Overview of OLED Displays. *Technology and Applications, OLED Microdisplays*. **2014**, 35–51.
4. Collison, C.; Treemanekarn, V.; Oldham, W.; Hsu, J.; Rothberg, L. Aggregation Effects on the Structure and Optical Properties of a Model PPV Oligomer. *Synthetic Metals*. **2001**, *119*, 515–518.
5. Andersson, M.; Yu, G.; Heeger, A. Photoluminescence And Electroluminescence of Films from Soluble PPV-Polymers. *Synthetic Metals*. **1997**, *85*, 1275–1276.
6. Yamaguchi, Y.; Tanaka, T.; Kobayashi, S.; Wakamiya, T.; Matsubara, Y.; Yoshida, Z.-I. Light-Emitting Efficiency Tuning Of Rod-Shaped  $\pi$  Conjugated Systems by Donor and Acceptor Groups. *J. Am. Chem. Soc. Journal of the American Chemical Society*. **2005**, *127*, 9332–9333.
7. Brunner, K.; Dijken, A. V.; Börner, H.; Bastiaansen, J. J. A. M.; Kiggen, N. M. M.; Langeveld, B. M. W. Carbazole Compounds As Host Materials for Triplet Emitters in Organic Light-Emitting Diodes: Tuning the HOMO Level without Influencing the Triplet Energy in Small Molecules. *J. Am. Chem. Soc. Journal of the American Chemical Society*. **2004**, *126*, 6035–6042.

8. Gong, Y.; Guo, X.; Wang, S.; Su, H.; Xia, A.; He, Q.; Bai, F. Photophysical Properties Of Photoactive Molecules with Conjugated Push–Pull Structures. *J. Phys. Chem. The Journal of Physical Chemistry A*. **2007**, *111*, 5806–581
9. Gupta, A.; Watkins, S. E.; Scully, A. D.; Singh, T. B.; Wilson, G. J.; Rozanski, L. J.; Evans, R. A. Band-Gap Tuning of Pendant Polymers for Organic Light-Emitting Devices and Photovoltaic Applications. *Synthetic Metals*. **2011**, *161*, 856–863.
10. Gong, Y.; Guo, X.; Wang, S.; Su, H.; Xia, A.; He, Q.; Bai, F. Photophysical Properties Of Photoactive Molecules with Conjugated Push–Pull Structures. *J. Phys. Chem.* **2007**, *111*, 5806–5812.
11. Patra, A.; Pan, M.; Friend, C. S.; Lin, T.-C.; Cartwright, A. N.; Prasad, P. N.; Burzynski, R. Electroluminescence Properties Of Systematically Derivatized Organic Chromophores Containing Electron Donor and Acceptor Groups. *Chemistry of Materials Chem. Mater.* **2002**, *14*, 4044–4048.
12. Basavaraja, J.; Inamdar, S.; Kumar, H. S. Solvents Effect on the Absorption and Fluorescence Spectra of 7-Diethylamino-3-Thenoylcoumarin: Evaluation and Correlation between Solvatochromism and Solvent Polarity Parameters. *Spectrochimica Acta Part A: Molecular and Biomolecular Spectroscopy*. **2015**, *137*, 527–534.
13. Zhang, C.; Kang, S.; Ma, X.; Xiao, G.; Yan, D. Synthesis And Characterization of Sulfonated Poly(Arylene Ether Phosphine Oxide)s with Fluorenyl Groups by Direct Polymerization for Proton Exchange Membranes. *Journal of Membrane Science*. **2009**, *323*, 99–105.

14. Smith, C. D.; Grubbs, H.; Webster, H.F.; Gungor, A.; Wightman, J. P.; McGrath, J. E. Unique Characteristics Derived from Poly(Arylene Ether Phosphine Oxide)s. *High Performance Polymers*. **1991**, 3, 211–229.
15. Andrejevic, M.; Schmitz, J.; Fossum, E. Poly(Arylene Ether)s Derived from N-Alkyl-N-Phenyl-3,5-Difluorobenzene Sulfonamides: Effect of Alkyl Chain Length on the Glass Transition Temperature. *Materials Today Communications*. **2015**, 3, 10–16.
16. Beek, D. V.; Fossum, E. Linear Poly(Arylene Ether)s with Pendant Benzoyl Groups: Geometric Isomers of PEEK or Substituted Poly(Phenylene Oxide) *Macromolecules*. **2009**, 42, 4016–4022.
17. Kaiti, S.; Himmelberg, P.; Williams, J.; Abdellatif, M.; Fossum, E. Linear Poly(arylene ether)s with Pendant Phenylsulfonyl Groups: Nucleophilic Aromatic Substitution Activated from the Meta Position. *Macromolecules* **2006**, 39, 7909-7914.
18. Hedrick, J. L. Poly(aryl ether benzothiazole)s. *Macromolecules*. **1991**, 24, 6361–6364.
19. Hilborn, J. G.; Labadie, J. W.; Hedrick, J. L. Poly(aryl ether-benzoxazole)s. *Macromolecules*. **1990**, 23, 2854–2861.
20. Hedrick, J. L.; Jonsson, H.; Carter, K. R. Poly(Aryl Ether)s Containing Pendent Benzoxazole and Benzothiazole Units. *Macromolecules*. **1995**, 28, 4340–4343.
21. Huang L, H. *Hydroquinone-based poly(arylene ether)s with pendent benzothiazole or benzoxazole and 3-sulfonated phenyl sulfonyl groups for use as proton exchange membranes*. masters, wright state university, **2013**.

22. So, Y.-H.; Heeschen, J. P. Mechanism Of Polyphosphoric Acid and Phosphorus Pentoxide–Methanesulfonic Acid as Synthetic Reagents for Benzoxazole Formation. *The Journal of Organic Chemistry J. Org. Chem.* **1997**, *62*, 3552–3561.
23. Kashiyama, E.; Hutchinson, I.; Chua, M.-S.; Stinson, S. F.; Phillips, L. R.; Kaur, G.; Sausville, E. A.; Bradshaw, T. D.; Westwell, A. D.; Stevens, M. F. G. Antitumor Benzothiazoles. 8. 1 Synthesis, Metabolic Formation, And Biological Properties of the C - and N -Oxidation Products of Antitumor 2-(4-Aminophenyl)Benzothiazoles . *J. Med. Chem. Journal of Medicinal Chemistry.* **1999**, *42*, 4172–4184.
24. Irma Goldberg, "Ueber Phenylirungen bei Gegenwart von Kupfer als Katalysator". *Berichte der deutschen chemischen Gesellschaft*, **1906**. 39 (2): 1691–1692.
25. Zhang, H.; Cai, Q.; Ma, D. Amino Acid Promoted CuI-Catalyzed C–N Bond Formation Between Aryl Halides and Amines or N-Containing Heterocycles. *The Journal of Organic Chemistry J. Org. Chem.* **2005**, *70*, 5164–5173.